doi.org/10.26434/chemrxiv.7105715.v1

Dynamics of Individual Molecular Shuttles Under Mechanical Force

Teresa Naranjo, Kateryna Lemishko, Sara de Lorenzo, Alvaro Somoza, Felix Ritort, Emilio Pérez, Borja Ibarra

Submitted date: 10/10/2018 • Posted date: 10/10/2018

Citation information: Naranjo, Teresa; Lemishko, Kateryna; Lorenzo, Sara de; Somoza, Alvaro; Ritort, Felix; Pérez, Emilio; et al. (2018): Dynamics of Individual Molecular Shuttles Under Mechanical Force. ChemRxiv. Preprint.

Here, we exploit the high force (0.1 pN), spatial (1 nm) and temporal (1 kHz) resolutions of optical tweezers to quantify and control mechanically the real-time kinetics of individual synthetic molecular shuttles operating at near-physiological conditions, for several hundreds of switching cycles, near equilibrium conditions.

File list (2)

Dynamics of individual molecular shuttles under mechanical force

Teresa Naranjo[1, †], Kateryna M. Lemishko[2, †], Sara de Lorenzo[1], Álvaro Somoza[1,2], Felix Ritort[3,4], Emilio M. Pérez[1*] and Borja Ibarra[1,2*]

[1]IMDEA Nanociencia, C/Faraday 9, Ciudad Universitaria de Cantoblanco, 28049, Madrid, Spain.

[2] Nanobiotecnología (IMDEA-Nanociencia) Unidad Asociada al Centro Nacional de Biotecnología (CSIC) 28049, Madrid, Spain.

[3] Condensed Matter Physics Department, University of Barcelona, C/Marti i Franques s/n, 08028 Barcelona, Spain

[4] CIBER-BBN de Bioingeniería, Biomateriales y Nanomedicina, Instituto de Sanidad Carlos III, Madrid, Spain

*Correspondence to: emilio.perez@imdea.org, borja.ibarra@imdea.org

†T. Naranjo and K. M. Lemishko contributed equally to this work.

Recent advances in synthetic molecular machinery have led to systems with the ability to work as molecular motors [1,2]. The kinetics and thermodynamics behind the operation of some of these molecular devices in bulk are well understood. However, quantitative information on the dynamics of individual synthetic molecular devices is still lacking [3]. Single molecule force spectroscopy techniques have revolutionized our understanding of biological motors [4,5], but they

have not had impact on the field of synthetic molecular machines. There are some examples of measurements of synthetic molecular devices at the single-molecule level using AFM[6-10], but they could not access the thermally-induced dynamics governing their operation. Here, we exploit the high force (0.1 pN), spatial (1 nm) and temporal (1 kHz) resolutions of optical tweezers[4,11] to quantify and control mechanically the real-time kinetics of individual synthetic molecular shuttles operating at near-physiological conditions, for several hundreds of switching cycles, near equilibrium conditions.

In molecular shuttles, a macrocycle trapped onto a linear component (thread) can be moved reversibly between two or more portions of the thread (stations), in response to external stimuli. These architectures are the basis for some of the most advanced examples of synthetic molecular machines [12-16]. Our system comprises a hydrogen-bonded Leigh-type molecular shuttle, featuring a tetraamide macrocycle locked onto a oligoethyleneglycol thread by two diphenylethyl groups (stoppers) situated at either end of the axle, Fig. 1A. The thread features fumaramide (*fum*) and succinic amide-ester (*succ*) stations, each of which can establish up to four hydrogen bonds with the macrocycle with sufficiently different affinities to yield a *fum:succ* occupancy ratio biased towards the *fum* station, even in the strongly competing solvent d_6-DMSO (Supplementary Materials). To interface the synthetic device with the optical tweezers, a single shuttle was connected between two functionalized beads using two double-stranded DNA (dsDNA) molecules, Fig. 1B. The first dsDNA connects the macrocycle with the bead in the optical trap and serves as a handle to control and trace the stochastic motion of the macrocycle between the two stations. The second dsDNA connects the stopper adjacent to the *fum* station to a bead on top of a micropipette, providing physical separation (~282 nm) between them. Experiments were

performed under aqueous conditions (20 mM Tris-HCl pH 7.5, 150 mM NaCl) at 22±1 °C.

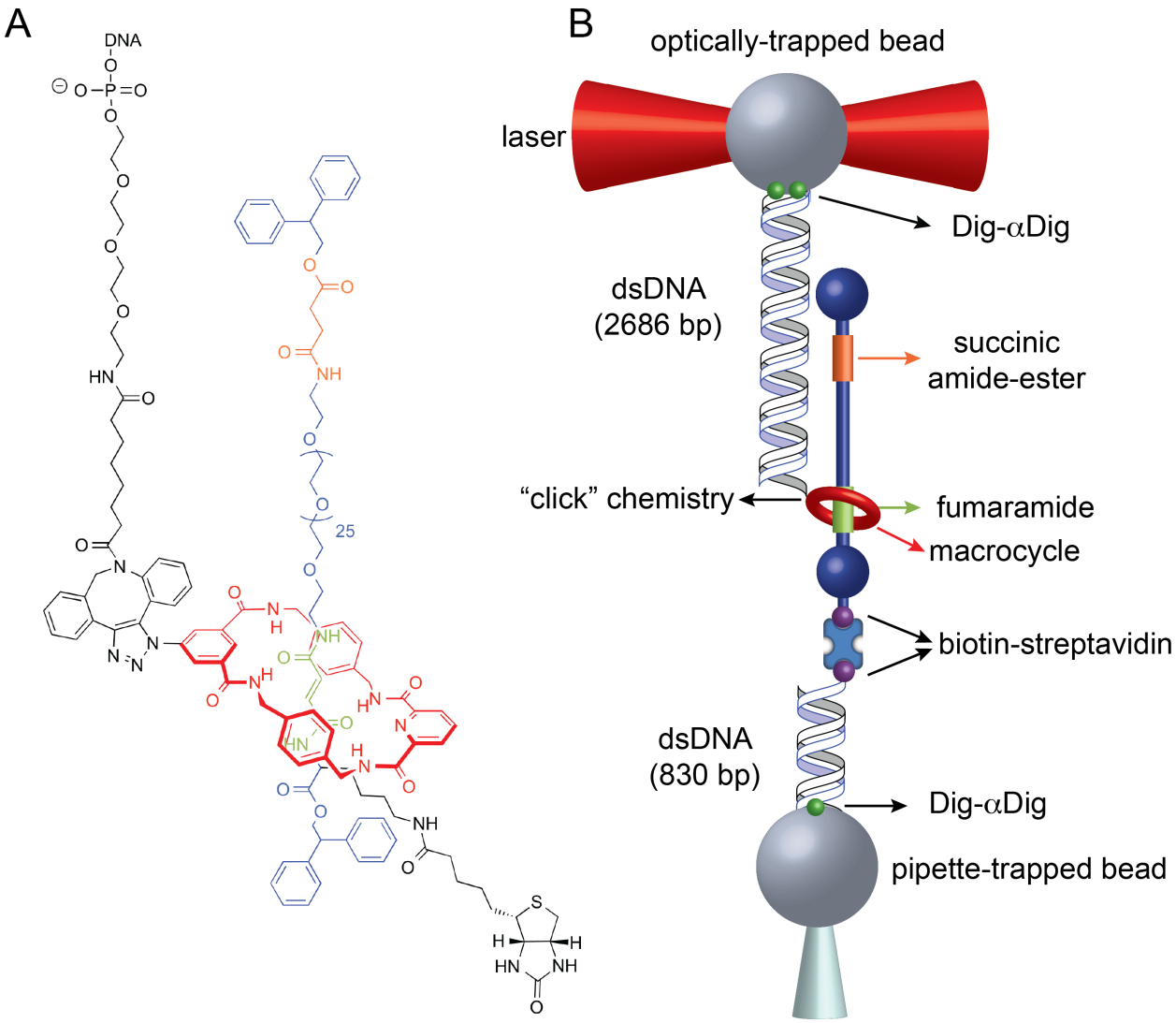

Fig. 1. Molecular design and experimental set-up. (**A**) The chemical structure of the molecular shuttle consists of a benzylic tetraamide macrocycle (red) locked onto an axle (blue) terminated by diphenylethyl groups at each end (stoppers). The axle contains fumaramide (*fum*, green) and succinic amide-ester (*succ*, orange) stations separated by a long oligoethyleneglycol spacer. At low forces the macrocycle resides predominantly over the *fum* station. A DNA oligonucleotide was covalently attached to the macrocycle to allow for manipulation in the optical tweezers. (**B**) The molecular shuttle is attached to two polystyrene beads through two dsDNA molecules (not

to scale): The 2686 bp dsDNA molecule connects the macrocycle to the bead in the optical trap via digoxigenin-antidigoxigenin (Dig-αDig) connections. The 830 bp dsDNA molecule connects the shuttle to a bead held by suction on a micropipette, via biotin-streptavidin connections at one end and Dig-αDig at the other end (Supplementary Materials). Load is applied to the system by moving the optical trap away from the micropipette. At constant load, the shuttling dynamics of the macrocycle are inferred by measuring the motions of the bead in the optical trap.

In order to investigate the mechanical strength of the interaction of the macrocycle at each station, individual rotaxane-DNA hybrids were subjected to pulling-relaxing cycles by moving the optical trap relative to the micropipette at a fixed pulling rate of 200 nm s^{-1} (Fig. 2A). At low pulling forces, the force-extension curves fit well to a worm-like chain model (WLC) of a polymer with a persistence length of 50 nm, characteristic of a single dsDNA molecule [17]. At these forces, the macrocycle resides over the thermodynamically preferred *fum* station. Once the force exceeds the strength of the noncovalent interactions holding the macrocycle at the *fum* station, an abrupt increase in extension is observed. Using the WLC model, we calculate the additional contour length released during this transition, ΔL_c. The average ΔL_c was 15 ± 2 nm, which is consistent with the calculated distance between stations in the fully extended shuttle (11.2 nm, Fig. S1), an unambiguous confirmation that the peak corresponds to the force-induced shuttling of the macrocycle from *fum* to *succ* stations. When relaxing the force, a sudden extension decrease to the original position is observed, that reflects the ability of the macrocycle to exert a force against the load to return to the thermodynamically favored *fum* station [10]. The robustness of our system allows the collection of up to one hundred force-extension curves of each rotaxane-DNA hybrid (Fig. S2) and the construction of detailed histograms for the rupture forces at each station (Fig. 2B). The average rupture forces are f_{fum} = 8.8 ± 0.6 pN and f_{succ} = 8.1

± 0.5 pN (Fig. 2B), which are comparable with those required to break an equivalent number of H-bonds in DNA and RNA hairpins under similar conditions [18]. In addition, the intersection of the force distributions denotes the coexistence force, $f_{1/2,}$ or the force under which the macrocycle has an equal probability of residing over the *fum* or *succ* stations, $f_{1/2}$ = 8.46 pN. In contrast to previous studies [6-10], this is a near-equilibrium measurement, so the product of the coexistence force, $f_{1/2,}$ and ΔL_c allows us to obtain directly $\Delta G = 30.8 \pm 2\ k_BT$ (18.5 ± 2 kcal mol^{-1}) [11]. ΔG equals the free energy of shuttling from the *fum* to the *succ* station at zero force plus the free energy for stretching the rotaxane-DNA hybrid from a force of 0 pN to $f_{1/2}$, which we measured as 11.8 k_BT (7.1 kcal mol^{-1}, Fig. S3). Therefore, the free energy of shuttling of the macrocycle from the *fum* to the *succ* station at zero force under near-physiological conditions is 19 ± 2 k_BT (11.4 ± 2 kcal mol^{-1}).

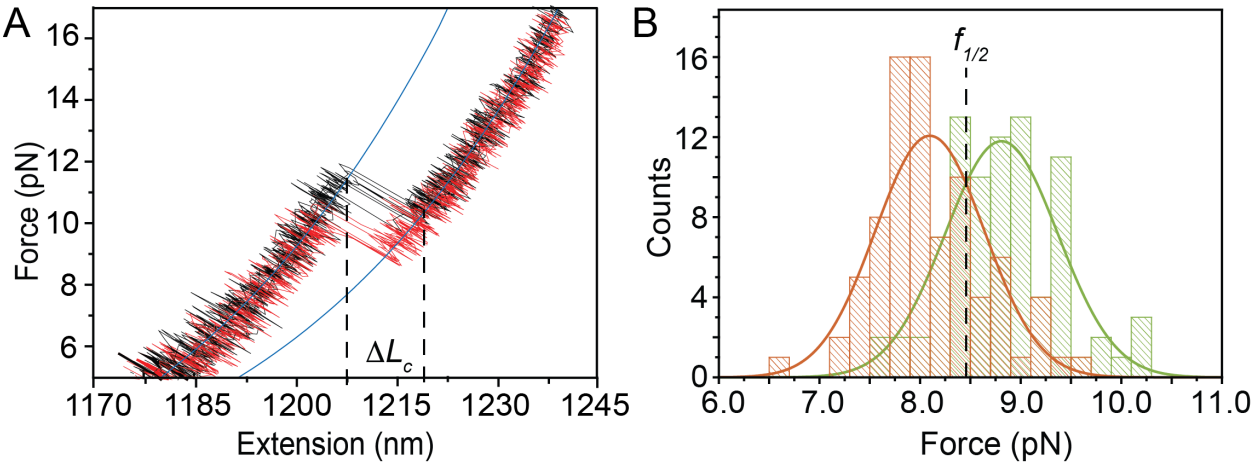

Fig. 2. **Pulling-relaxing experiments.** (**A**) Representative pulling (black) and relaxing (red) curves (N=6) recorded at a pulling rate of 200 nm s^{-1} displaying WLC behavior of dsDNA handles (blue line). WLC fit to the contour length increase after the shuttling event gives ΔLc ~15 nm. (**B**) The intersection of the distributions of the breaking forces at *fum* (orange Gaussian fit) and *succ* (green Gaussian fit) stations reveals the coexistence force, $f_{1/2}$ = 8.46 pN (N = 450

curves).

In order to investigate the dynamics and bi-stability of the system we impose a constant force around $f_{1/2}$ with a feed-back stabilized protocol capable of maintaining a preset force within ~0.05 pN. Under these conditions, hundreds of shuttling events of the macrocycle between the two stations were monitored in real-time during minutes (Fig. 3A and Fig. S4). These shuttling events present well defined residence times at each station, in which the macrocycle undergoes thermal motion near one station, and much faster transition times from one station to the other, a finding consistent with models [19] (Fig. 3B). The residence times were exponentially distributed, as expected for a two-state system close to equilibrium (Fig. S5) [20]. At forces ~ $f_{1/2}$ (Fig. 3, middle column), the macrocycle spends roughly equal amounts of time at each station. The histogram of extensions shows two similar peaks, which fit well to two Gaussian curves separated by an averaged Δx = 15.5 ± 2.5 nm (Fig. 3C), identical to the contour length increase after the shuttling event measured in the pulling-relaxing experiments. By gradually varying the force on the system, it was possible to displace the equilibrium favoring occupancy of either the *fum* or *succ* bound states (Fig.3 left and right columns). From the extension histograms at different forces, we obtain directly the energy profiles, using Boltzmann's distribution (Fig. 3D). Within the force range studied, the profiles show a well-defined transition state between two broad minima, the relative depth of which varies with force.

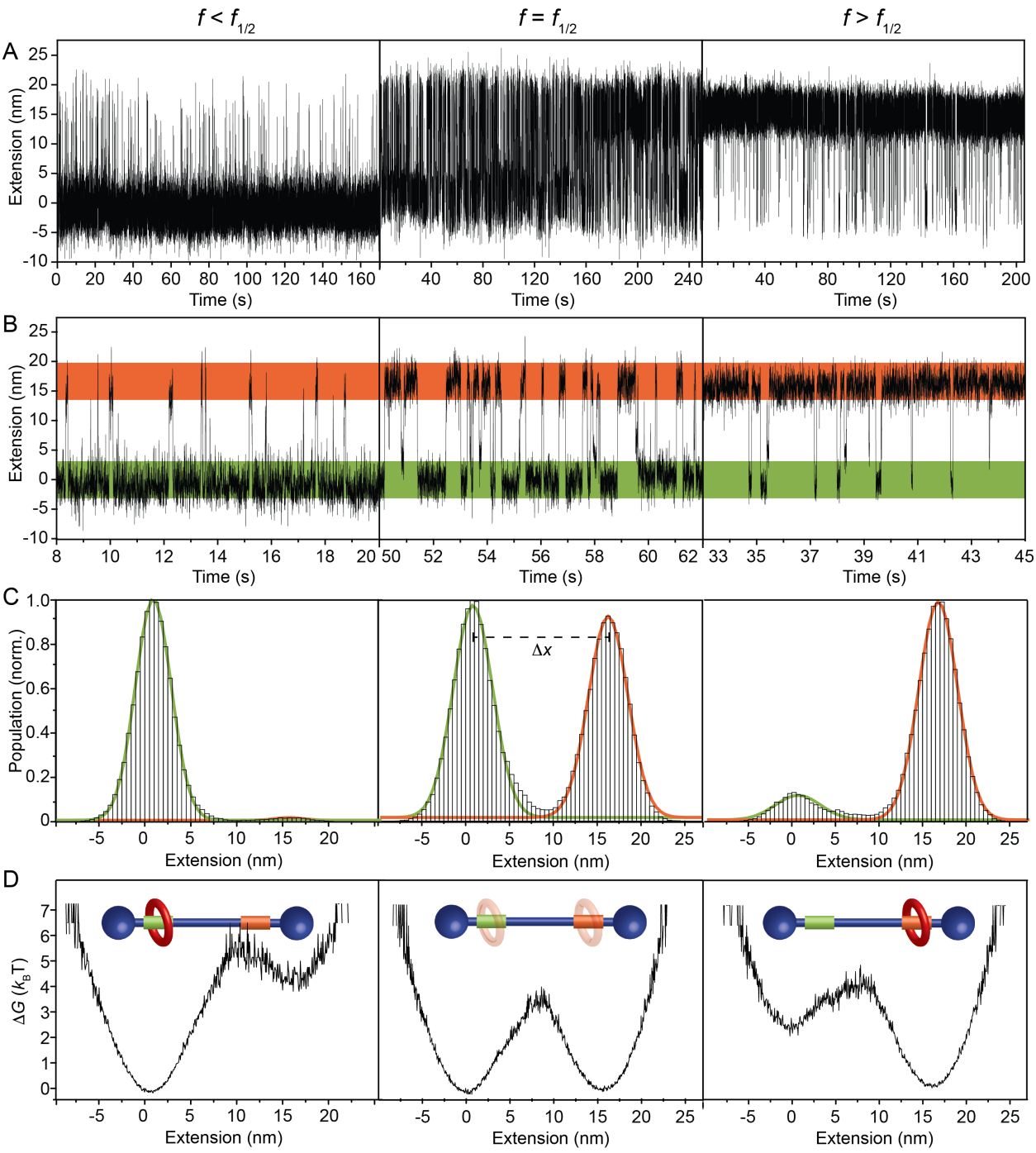

Fig. 3. **Shuttling dynamics, positional control and energy profiles.** (**A**) Extension vs. time data for single molecular shuttles at different constant forces. (**B**) Zoom-in on the data presented in A at arbitrary time intervals, showing residence and transition times. (**C**) Extension histograms, fitted with two Gaussian curves (orange and green lines) affording a shuttling

distance of Δx~15 nm. (**D**) Energy profiles at each force, obtained directly from the relative populations depicted in **C**. At force $<f_{1/2}$ the macrocycle occupies preferentially the *fum* station (8.1 pN, left column). At force ~$f_{1/2}$ both stations present similar occupancies (8.5 pN, middle column). At force $>f_{1/2}$ the macrocycle occupies preferentially the *succ* station (9.6 pN, right column).

To investigate the force dependence of the shuttling rates (inverse of residence times) from *fum* to *succ* station, k_{fum}, and its reverse k_{succ}, we measure the rates of shuttling of 24 different molecular shuttles at several constant forces around $f_{1/2}$ (Fig. 4). The experimental values of k_{fum} and k_{succ} present an exponential dependence on force and fit well to the Bell-Evans model [21-24] along the entire range of forces measured, confirming again that the shuttling occurs near equilibrium conditions (Fig. 4). From the fits, we can extract the main parameters that characterize the free energy landscape of the shuttling process (Supplementary Materials). The intersection of the two linear fits rendered the coexistence force, $f_{1/2}$= 8.83 pN, which is consistent with the $f_{1/2}$ value obtained from the rupture force distributions in the pulling-relaxing experiments. This value, together with the average shuttling distance measured between the two stations in these experiments, Δx = 15.5 ± 2.5 nm, yield ΔG = 33 ± 2 k_BT (20 ± 2 kcal mol^{-1}). These experiments corroborate the value for ΔG obtained with the pulling-relaxing experiments. In addition, the results of the fits rendered the relative distances from the *fum* and *succ* stations to the transition state at $f_{1/2}$, x_{fum}= 10 ± 2 nm and x_{succ}= 6 ± 2 nm, respectively. Therefore, for these particular experimental conditions, the distance to the transition state at the coexistence force is asymmetric: the macrocycle needs to travel a longer distance to reach the point where the probability of completing the shuttling process is 50% after abandoning the stronger *fum* station, compared to the weaker *succ* station.

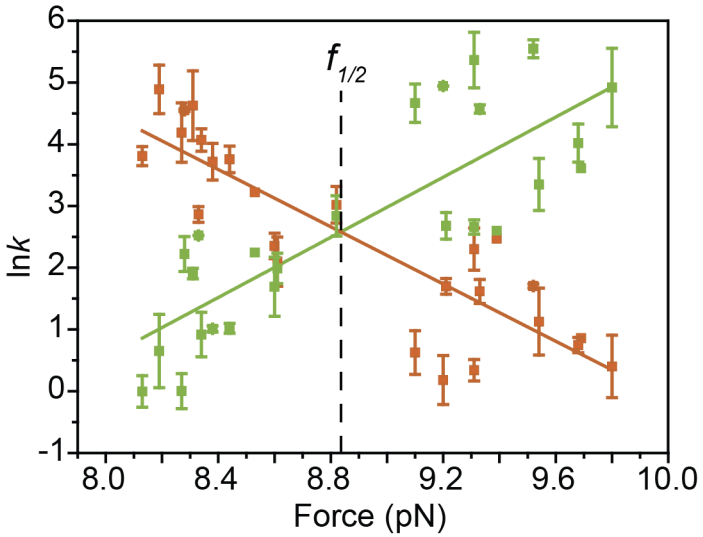

Fig. 4. Dependence of shuttling rates with force. The shuttling rates from *fum* to *succ* station, k_{fum} (green), and the backward rates, k_{succ} (orange), vary exponentially with force. Fits of the data with the Bell-Evans theory revealed the coexistence force, $f_{1/2}$, and the main parameters of the energy landscape.

In summary, our experimental design allowed the measurement of hundreds of pulling-relaxing cycles and hundreds of real-time shuttling events on tens of individual molecular shuttles. From these data, we obtain crucial information that is not accessible from bulk experiments, such as the mechanical stability of the macrocycle at each station, the dynamics of shuttling, and a clear picture of the energy landscape at different forces, which reveals broad energy minima separated by a well-defined transition state, positioned asymmetrically with respect to each station. This experimental picture is significantly different from idealized theoretical energy profiles.[25]

The experimental system will enable the study of the combined effect of force and other variables (temperature, light, solvent composition) on the operation of individual molecular

shuttles under aqueous conditions. The results from these studies will facilitate more reliable comparisons with biological devices (also operating in water) and, therefore, help to design more efficient synthetic and hybrid molecular devices. From a more general point of view, once the synthetic and technological challenges to study the thermodynamics and real time kinetics of individual synthetic molecular devices have been surmounted, the atomic precision of synthetic chemistry will allow addressing fundamental questions such as the structural basis for microscopic reversibility or the controversial presence (or absence) of quantum effects in nanoscopic engines [26].

References

1 Erbas-Cakmak, S., Leigh, D. A., McTernan, C. T. & Nussbaumer, A. L. Artificial Molecular Machines. *Chem. Rev.* **115**, 10081-10206, doi:10.1021/acs.chemrev.5b00146 (2015).

2 Kassem, S. *et al.* Artificial molecular motors. *Chem. Soc. Rev.* **46**, 2592-2621, doi:10.1039/C7CS00245A (2017).

3 Pezzato, C., Cheng, C., Stoddart, J. F. & Astumian, R. D. Mastering the non-equilibrium assembly and operation of molecular machines. *Chem. Soc. Rev.* **46**, 5491-5507, doi:10.1039/C7CS00068E (2017).

4 Moffitt, J. R., Chemla, Y. R., Smith, S. B. & Bustamante, C. Recent Advances in Optical Tweezers. *Annu. Rev. Biochem.* **77**, 205-228, doi:10.1146/annurev.biochem.77.043007.090225 (2008).

5 Neuman, K. C. & Nagy, A. Single-molecule force spectroscopy: optical tweezers, magnetic tweezers and atomic force microscopy. *Nat. Methods* **5**, 491, doi:10.1038/nmeth.1218 (2008).

6 Sluysmans, D. *et al.* Synthetic oligorotaxanes exert high forces when folding under mechanical load. *Nat. Nanotechnol.* **13**, 209-213 (2018).

7 Hanozin, E. *et al.* Where Ion Mobility and Molecular Dynamics Meet To Unravel the (Un)Folding Mechanisms of an Oligorotaxane Molecular Switch. *ACS Nano* **11**, 10253-10263, doi:10.1021/acsnano.7b04833 (2017).

8 Sluysmans, D., Devaux, F., Bruns, C. J., Stoddart, J. F. & Duwez, A.-S. Dynamic force spectroscopy of synthetic oligorotaxane foldamers. *Proc. Natl. Acad. Sci. USA* (2017).

9 Van Quaethem, A., Lussis, P., Leigh, D. A., Duwez, A.-S. & Fustin, C.-A. Probing the mobility of catenane rings in single molecules. *Chem. Sci.* **5**, 1449-1452, doi:10.1039/c3sc53113a (2014).

10 Lussis, P. *et al.* A single synthetic small molecule that generates force against a load. *Nat. Nanotechnol.* **6**, 553-557, doi:10.1038/nnano.2011.132 (2011).

11 Tinoco Jr, I. & Bustamante, C. The effect of force on thermodynamics and kinetics of single molecule reactions. *Biophys. Chem.* **101-102**, 513-533, doi:https://doi.org/10.1016/S0301-4622(02)00177-1 (2002).

12 Serreli, V., Lee, C.-F., Kay, E. R. & Leigh, D. A. A molecular information ratchet. *Nature* **445**, 523-527 (2007).

13 Lewandowski, B. *et al.* Sequence-Specific Peptide Synthesis by an Artificial Small-Molecule Machine. *Science* **339**, 189-193, doi:10.1126/science.1229753 (2013).

14 Cheng, C. *et al.* An artificial molecular pump. *Nat. Nanotechnol.* **10**, 547-553, doi:10.1038/nnano.2015.96 (2015).

15 Berna, J. *et al.* Macroscopic transport by synthetic molecular machines. *Nat. Mater.* **4**, 704-710 (2005).
16 De Bo, G. *et al.* An artificial molecular machine that builds an asymmetric catalyst. *Nat. Nanotechnol.* **13**, 381-385, doi:10.1038/s41565-018-0105-3 (2018).
17 Smith, S., Finzi, L. & Bustamante, C. Direct mechanical measurements of the elasticity of single DNA molecules by using magnetic beads. *Science* **258**, 1122-1126, doi:10.1126/science.1439819 (1992).
18 Bercy, M. & Bockelmann, U. Hairpins under tension: RNA versus DNA. *Nucleic Acids Res.* **43**, 9928-9936, doi:10.1093/nar/gkv860 (2015).
19 Astumian, R. D. Stochastically pumped adaptation and directional motion of molecular machines. *Proc. Natl. Acad. Sci. USA* (2018).
20 Carlos Bustamante, Yann R. Chemla, Nancy R. Forde, a. & Izhaky, D. Mechanical Processes in Biochemistry. *Annu. Rev. Biochem.* **73**, 705-748, doi:10.1146/annurev.biochem.72.121801.161542 (2004).
21 Bell, G. Models for the specific adhesion of cells to cells. *Science* **200**, 618-627, doi:10.1126/science.347575 (1978).
22 Evans, E. Probing the Relation Between Force—Lifetime—and Chemistry in Single Molecular Bonds. *Annu. Rev. Biophys. Biomol. Struct.* **30**, 105-128, doi:10.1146/annurev.biophys.30.1.105 (2001).
23 Evans, E. & Ritchie, K. Dynamic strength of molecular adhesion bonds. *Biophys. J.* **72**, 1541-1555 (1997).
24 Merkel, R., Nassoy, P., Leung, A., Ritchie, K. & Evans, E. Energy landscapes of receptor–ligand bonds explored with dynamic force spectroscopy. *Nature* **397**, 50, doi:10.1038/16219 (1999).
25 Kay, E. R., Leigh, D. A. & Zerbetto, F. Synthetic molecular motors and mechanical machines. *Angew. Chem., Int. Ed.* **46**, 72-191 (2007).
26 Merali, Z. The new thermodynamics: how quantum physics is bending the rules. *Nature* **551**, 20-22 (2017).

Acknowledgments: We thank J. M. R. Parrondo, P. J. de Pablo, I. A. Rodriguez and E. R. Kay for comments on preliminary versions of this article, and members of the E.M. Pérez and B. Ibarra labs for useful discussions.

Funding

This work was supported by the European Research Council (ERC-StG-MINT 307609), the Ministerio de Economía y Competitividad (grants BFU2015-63714-R, CTQ2014-60541-P, SAF2014-56763-R, FIS2016-80458- P). IMDEA Nanociencia acknowledges support from the 'Severo Ochoa' Programme for Centres of Excellence in R&D (MINECO, Grant SEV-2016-0686). K.M.L was supported by the Ministerio de Educación Cultura y Deporte (FPU2014/06867). F.R. acknowledges support from ICREA Academia 2013.

Author contributions:

E.M.P and B.I. conceived, designed and directed the study. T.N. performed the chemical synthesis and K.M.L. the single molecule experiments. T.N. and K.M.L. analyzed the data. F.R. led data analysis and interpretation. A.S. and S.d.L. supplied analytical and technical tools. E.M.P and B.I. wrote the paper, with contributions from all authors.

Competing interests: The authors declare no competing interests.

Data and materials availability: Data and materials available upon request.

Supplementary Materials for

Dynamics of individual molecular shuttles under mechanical force

Teresa Naranjo, Kateryna M. Lemishko, Sara de Lorenzo, Álvaro Somoza, Félix Ritort, Emilio M. Pérez and Borja Ibarra.

Correspondence to: emilio.perez@imdea.org borja.ibarra@imdea.org

This PDF file includes:

S1 Materials and methods.

S1.1 Chemical synthesis of the molecular shuttle

The chemical structure of the shuttle comprises a strong binding station, namely fumaramide (green in Fig. 1A), which is known to be the best fit for a tetraamide macrocycle, because its two amide carbonyls are held by the *trans* double bond in the correct geometry to form four strong hydrogen bonds with the macrocycle. Separated by an oligoethyleneglycol spacer of approximately 15 nm in length (see below) we placed a succinic amide-ester station, (orange in Fig. 1A). This station shows less affinity for the macrocycle than the fumaramide station, due to its flexibility and the substitution of one of the amides with an ester, which is a significantly weaker H-bond acceptor. At the ends of the polar spacer two bulky diphenylethyl groups serve as stoppers to prevent unthreading of the macrocycle. One of the stopper ends is branched to include a biotin group. The synthesis of the thread for the shuttle was carried out in 12 steps (see below). Macrocyclization around the fumaramide station was performed using a purposely synthesized U-shape (compound III-14) The macrocycle contains an azide-decorated isophthalic acid chloride derivative (compound III-13) at a single position for the covalent attachment of a polydT oligonucleotide.

General. All solvents were dried according to standard procedures. Reagents were used as purchased. All air-sensitive reactions were carried out under argon atmosphere. Flash chromatography was performed using silica gel (Merck, Kieselgel 60, 230-240 mesh, or Scharlau 60, 230-240 mesh). Analytical thin layer chromatographies (TLC) were performed using aluminium-coated Merck Kieselgel 60 F254 plates. NMR spectra were recorded on a BrukerAvance 400 (^{1}H: 400 MHz; ^{13}C: 100 MHz; COSY: 400 MHz; HSQC: 400 MHz), spectrometer at 298 K, unless otherwise stated, using partially deuterated solvents as internal standards. Coupling constants (*J*) are denoted in Hz and chemical shifts (δ) in ppm. Multiplicities are denoted as follows: s = singlet, d = doublet, t = triplet, m = multiplet, br = broad. Fast Atom Bombardment (FAB) and Matrix-assisted Laser desorption ionization (coupled to a Time-Of-Flight analyzer) experiments (MALDI-TOF) were recorded on a VS AutoSpec spectrometer and a Bruker ULTRAFLEX III spectrometer, respectively.

Scheme of the rotaxane synthesis

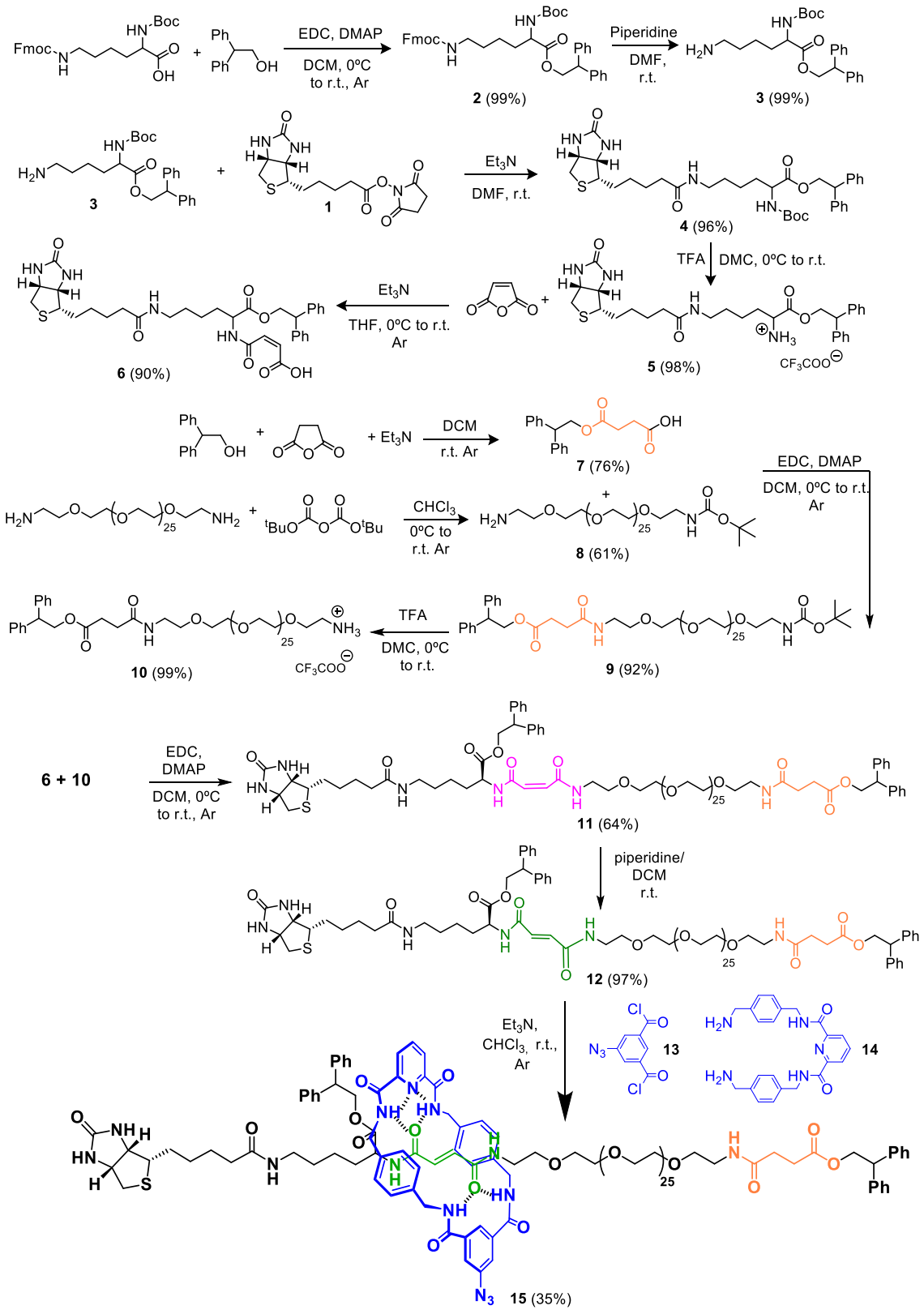

N-Hydroxysuccinimidobiotin

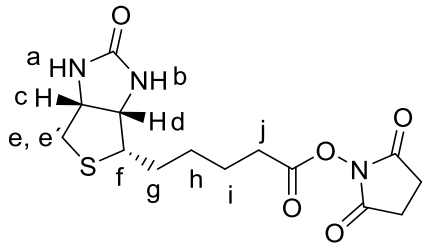

Compound 1

To a solution of D-biotin (75 mg, 0.31 mmol) and *N*-hydroxysuccinimide (39 mg, 0.34 mmol) in DMF, 1-ethyl-3-(3-dimethylaminopropyl)carbodiimide hydrochloride (EDCI) was added (71 mg, 0.37 mmol). After being stirred for 24h at room temperature, the reaction solution was concentrated to obtain a white solid. The white solid was washed by methanol several times to furnish compound **1** in a 90% yield (96mg, 0.28mmol). ^{1}H NMR ([D6]dimethyl sulfoxide): δ = 6.41 (s, 1H, H_a), 6.35 (s, 1H, H_b), 4.30 (m, 1H, H_c), 4.15 (m, 1H, H_d), 3.10 (m, 1H, H_f), 2.83 (dd, *J* = 5.1, 12.5 Hz, 1H, H_e or $H_{e'}$), 2.81 (s, 4H, succinimida-H), 2.67 (t, *J* = 7.36 Hz, 2H, H_j), 2.58 (d, *J* = 12.4 Hz, 1H, $H_{e'}$ or H_e), 1.55 (m, 6H, H_h, H_i, H_j); ^{13}C NMR ([D6]dimethyl sulfoxide): δ = 173.3 (3C), 168.9, 162.7, 61.0, 59.2, 55.2, 30.0, 27.8, 27.6, 25.4 (2C), 24.3 ppm. These data is in concordance with *J. Med. Chem*. 52, **2009**, 7003-7013.

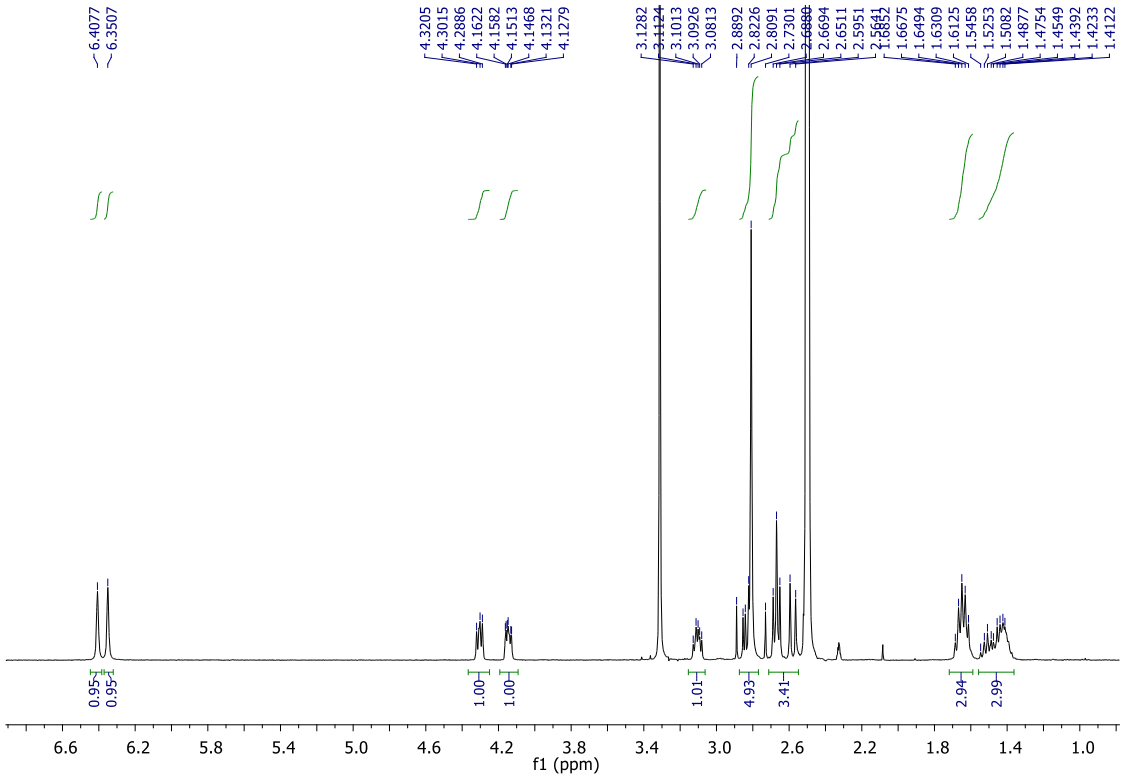
6.4077
6.3507
4.3205
4.3015
4.2886
4.1622
4.1582
4.1513
4.1468
4.1321
4.1279
3.1282
3.1124
3.1013
3.0926
3.0813
2.8892
2.8226
2.8091
2.7301
2.6694
2.6511
2.5951
1.6675
1.6494
1.6309
1.6125
1.5458
1.5253
1.5082
1.4877
1.4754
1.4549
1.4392
1.4233
1.4122
0.95
0.99
1.00
1.00
1.01
4.93
3.41
2.94
2.99
f1 (ppm)

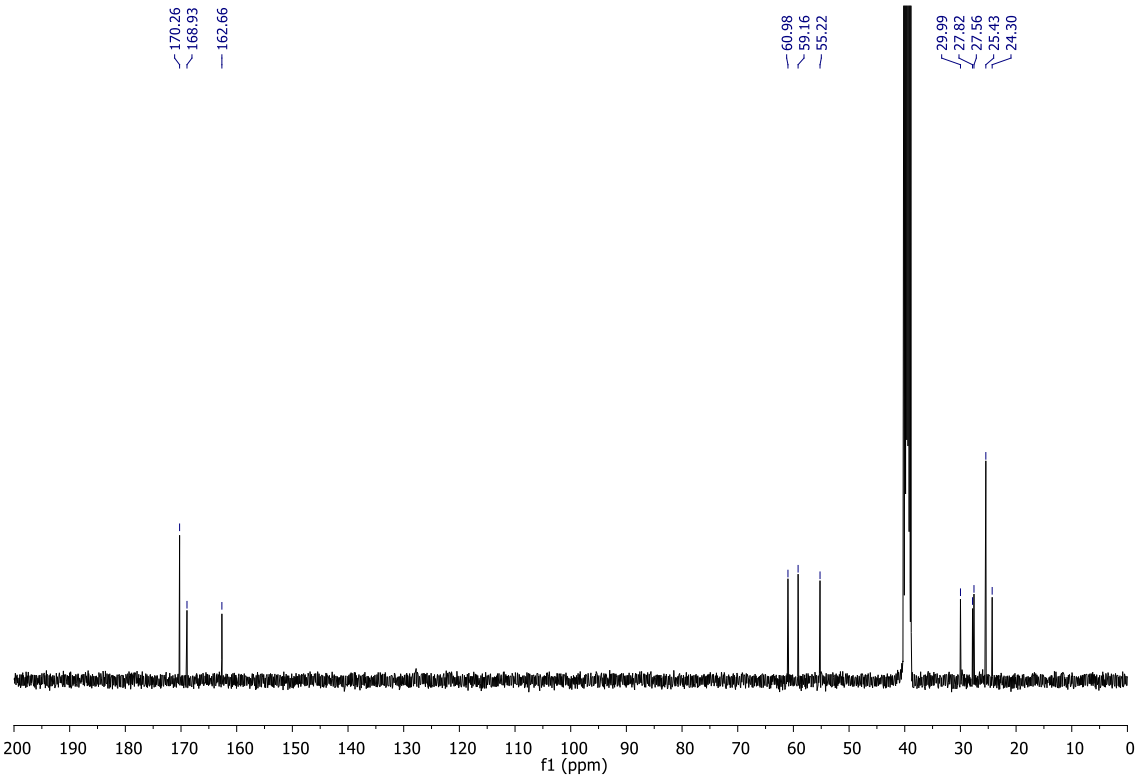
170.26
168.93
162.66
60.98
59.16
55.22
29.99
27.82
27.56
25.43
24.30
f1 (ppm)

2,2-diphenylethyl 6-([((9H-fluoren-9-yl)methoxy)carbonyl]amino)-2-[(*tert*-butoxy-carbonyl)amino)]hexanoate

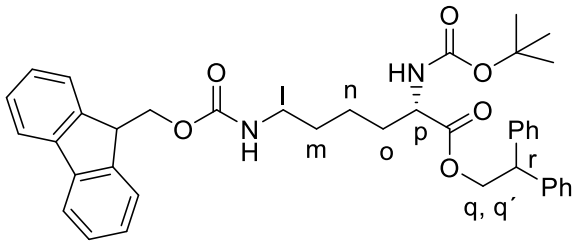

Compound 2

Boc-D-Lys(Fmoc)-OH (900 mg, 1.92 mmol) was dissolved in DCM (19 mL) and the solution was cooled to 0ºC, EDCI (732 mg, 3.84 mmol), 4-dimetylaminopyridine (DMAP) (catalytic amount) were added at 0ºC. The reaction mixture was allowed to stir at room temperature for 30 min, and then a solution of 2,2-diphenylethanol (457 mg, 2.3 mmol) in DCM (7.7 mL) was added to the activated acid. The reaction mixture was stirred overnight, concentrated under reduced pressure and then diluted with DCM. The organic layer was washed with 1M HCl, with $NaHCO_3$ (sat. aq.), then further washed with brine (sat. aq.), dried over Na_2SO_4 and concentrated under reduced pressure. The crude material was purified by column chromatography (eluent: hexane/AcOEt 3:1) to furnish the desired product as a colorless oil, 1.12g (quantitative yield). ^{1}H NMR ($CDCl_3$): δ = 7.77 (d, *J* = 7.5 Hz, 2H, Fmoc-H), 7.60 (d, *J* = 7.4 Hz, 2H, Fmoc-H), 7.40 (t, *J* = 8 Hz, 2H, Fmoc-H), 7.30 (m, 6 H, Ar-H), 7.22 (m, 6 H, Ar-H, Fmoc-H), 4.97 (m, 1 H, Fmoc-H), 4.80 (m, 1 H, H_q or $H_{q'}$), 4.68 (m, 1 H, NH), 4.58 (m, 1 H, H_q or $H_{q'}$), 4.41 (m, 3 H, H_r, CH_2-Fmoc), 4.22 (m, 2 H, H_p, NH), 3.05 (m, 2 H, H_l), 1.50 (m, 2H, H_m), 1.42 (s, 9 H, Boc-H), 1.07 (m, 2H, H_n); ^{13}C NMR ($CDCl_3$): δ= 172.5, 156.4, 155.3, 144.0 (2C), 141.3 (2C), 140.8, 140.6, 128.6 (2C), 128.6 (2C), 128.2 (2C), 128.1 (2C), 127.7 (2C), 127.0 (2C), 126.9 (2C), 125.0 (2C), 120.0 (2C), 79.9, 67.3, 66.4, 53.1, 49.8, 47.3, 40.6, 32.2, 29.7, 28.3, 22.1 (3C) ppm. MS m/z: calculated for $C_{40}H_{44}N_2O_6$ $[M+Na]^+$ 671.4 found MALDI-TOF 671.3.

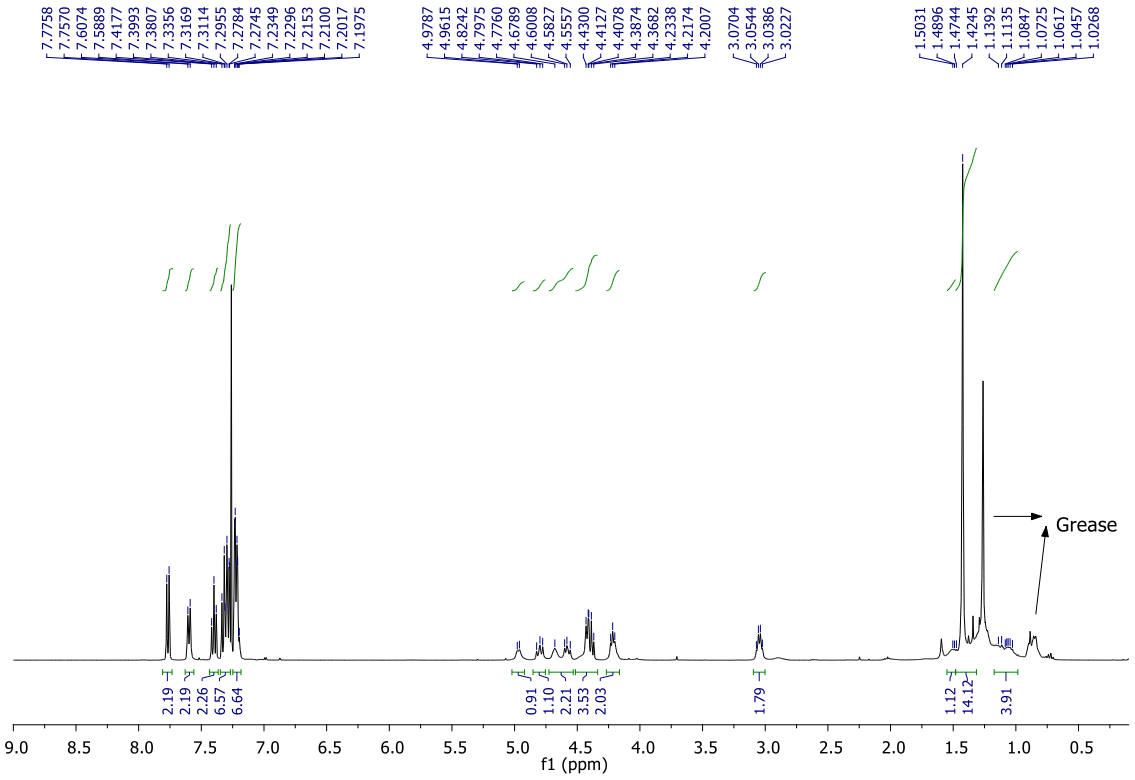
7.7758
7.7570
7.6074
7.5889
7.4177
7.3993
7.3807
7.3356
7.3169
7.3114
7.2955
7.2784
7.2745
7.2349
7.2296
7.2153
7.2100
7.2017
7.1975
4.9787
4.9615
4.8242
4.7975
4.7760
4.6789
4.6008
4.5827
4.5557
4.4300
4.4127
4.4078
4.3874
4.3682
4.2338
4.2174
4.2007
3.0704
3.0544
3.0386
3.0227
1.5031
1.4896
1.4744
1.4245
1.1392
1.1135
1.0847
1.0725
1.0617
1.0457
1.0268
Grease
2.19
2.19
2.26
6.57
6.64
0.91
1.10
2.21
3.53
2.03
1.79
1.12
14.12
3.91
f1 (ppm)

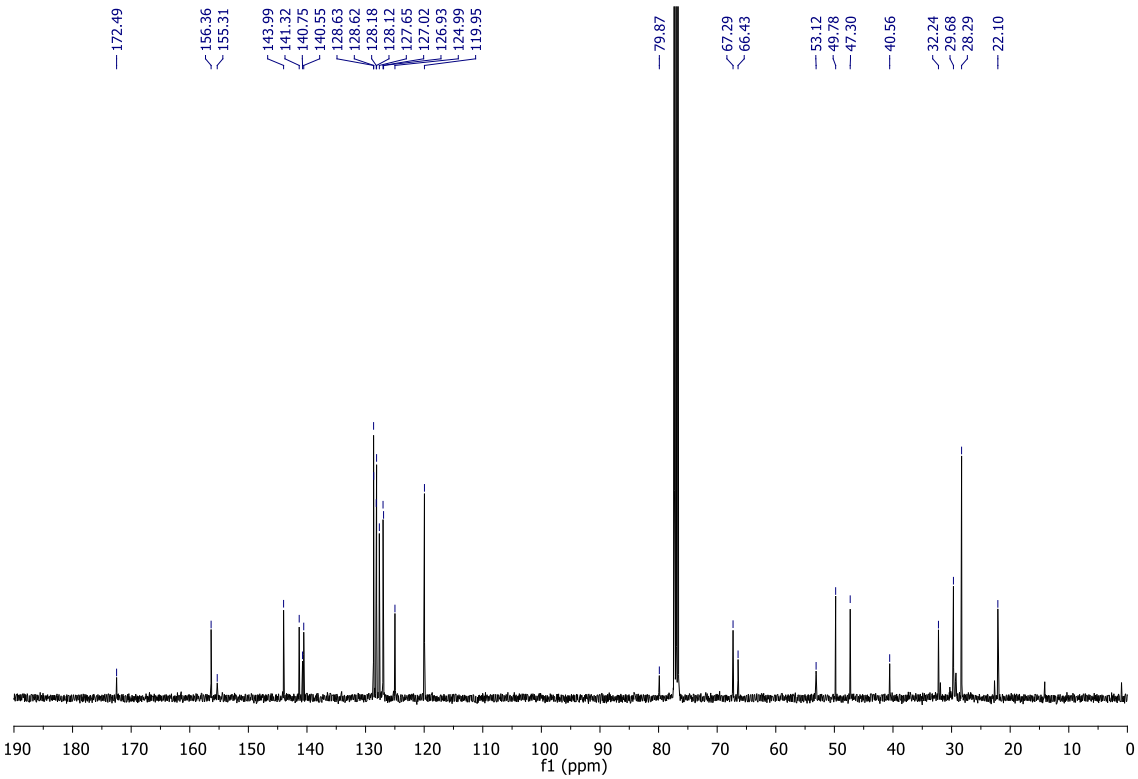
172.49
156.36
155.31
143.99
141.32
140.75
140.55
128.63
128.62
128.18
128.12
127.65
127.02
126.93
124.99
119.95
79.87
67.29
66.43
53.12
49.78
47.30
40.56
32.24
29.68
28.29
22.10
f1 (ppm)

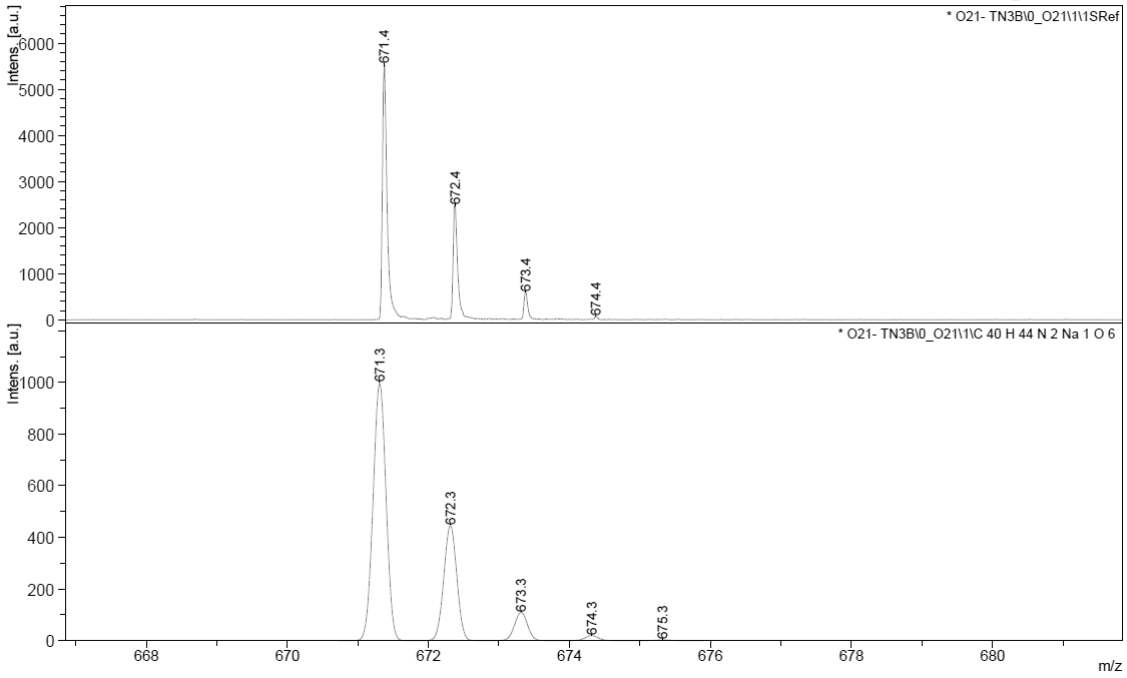

2,2-diphenylethyl 6-([((9H-fluoren-9-yl)methoxy)carbonyl]amino)-2-aminohexanoate

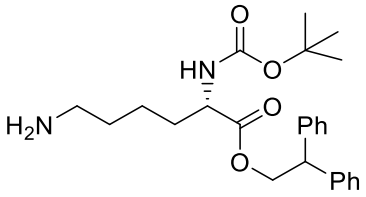

Compound 3

90mg (0.14 mmol) of compound **2** was dissolved in 1% pyridine and 1% DBU in DMF (2.8 mL). The reaction mixture was stirred for three hours at room temperature until the reaction was completed (TLC). The solvent was removed under reduced pressure to give compound **3** as yellowish oil (quantitative yield) and the crude material was used directly in the next step reaction.

2,2-diphenylethyl 2-[(tert-butoxycarbonyl)amino)-6-(biotinylamino] hexanoate

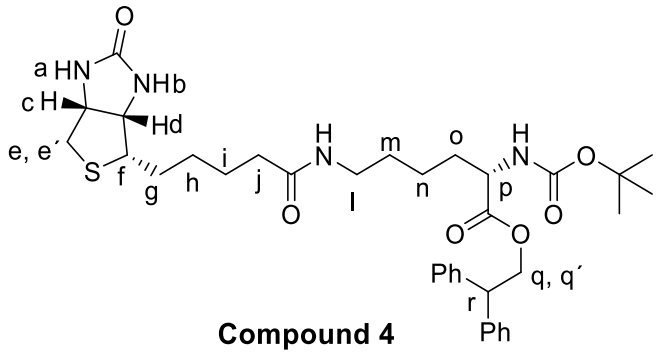

Compound 4

Compounds **3** (46 mg, 0.110 mmol) and **1** (25 mg, 0.073 mmol) were dissolved in DMF, and then Et_3N (20 μL, 0.144 mmol) was added. The reaction mixture was stirred overnight; then was concentrated in vacuum; the resulting residue was diluted in DCM and washed with water. The crude material was then purified by flash chromatography (using a gradient elution, from CH_3Cl to CH_3Cl/MeOH 9:1) to furnish **4** as a colorless oil, 45 mg, 96 %. ^{1}H NMR ($CDCl_3$): δ = 7.23 (m, 4 H, Ar-H), 7.14 (m, 6 H, Ar-H), 6.47 (br s, 1 H, H_a), 6.28 (br s, 1 H, H_b), 5.04 (br s, 1 H, NH), 4.71 (m, 1 H, , H_q or $H_{q'}$), 4.52 (dd, *J* = 7.3, 11.0 Hz, 1 H, $H_{q'}$ or H_q), 4.45 (dd, *J* = 4.8, 7.1 Hz, 1 H, H_c), 4.32 (t, *J* = 7.7 Hz, 1 H, H_r), 4.25 (dd, *J* = 4.5, 7.2 Hz, 1 H, H_d), 4.09 (br s, 1 H, H_p), 3.07 (m, 3 H, H_f, H_l), 2.83 (dd, *J* = 4.7, 12.9 Hz, 1 H, H_e or $H_{e'}$), 2.69 (d, *J* = 12.8 Hz, 1 H, $H_{e'}$ or $H_{e'}$), 2.17 (t, *J* = 6.8 Hz, 2 H, H_j), 1.61 (m, 4 H, H_g, H_i), 1.34 (s, 9 H, Boc-H), 1.11 (m, 8 H, H_h, H_n, H_m, H_o); ^{13}C NMR ($CDCl_3$): δ= 173.4, 172.6, 163.9, 155.5, 140.8, 140.6, 128.6 (2C), 128.6 (2C), 128.2 (2C), 128.1 (2C), 126.9 (2C), 79.9, 67.3, 61.9, 60.3, 55.6, 53.2, 49.8, 40.4, 39.1, 35.8, 32.2, 28.8, 28.3 (3C), 28.1, 28.0, 25.7, 22.4 ppm. MS m/z: calculated for $C_{35}H_{48}N_4O_6S$ $[M+Na]^+$ 675.3 found MALDI-TOF 675.4.

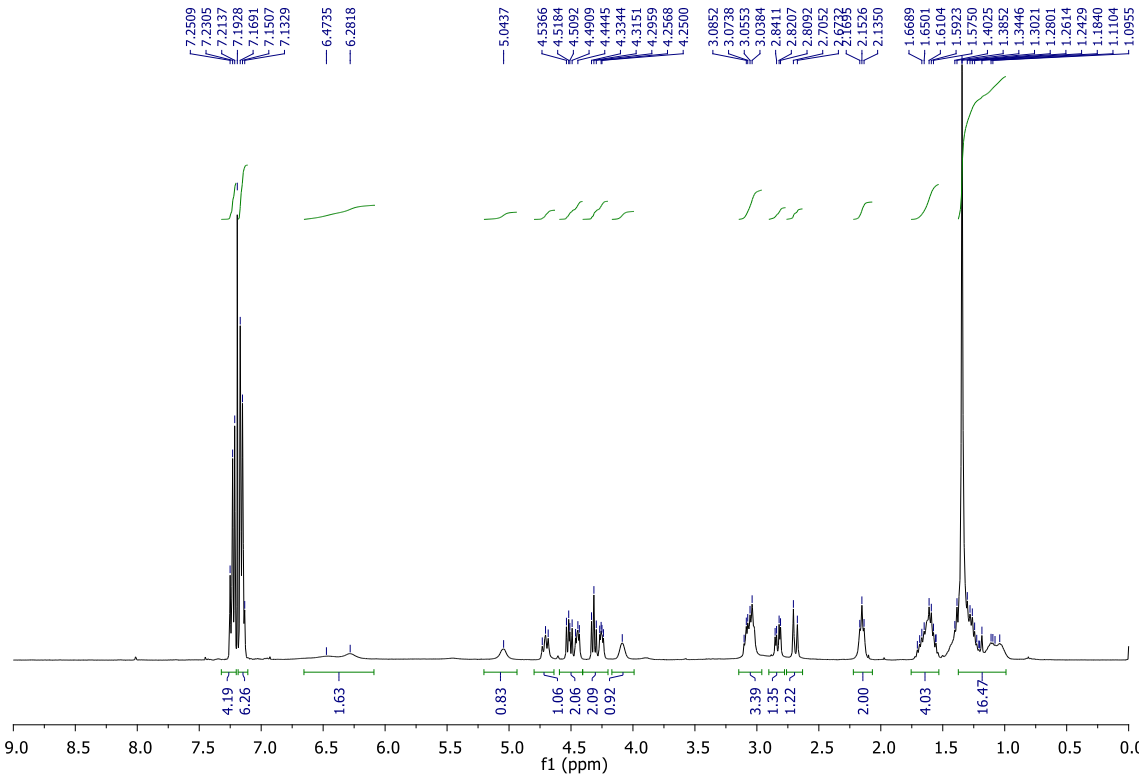
7.2509
7.2305
7.2137
7.1928
7.1691
7.1507
7.1329
6.4735
6.2818
5.0437
4.5366
4.5184
4.5092
4.4909
4.4445
4.3344
4.3151
4.2959
4.2568
4.2500
3.0852
3.0738
3.0553
3.0384
2.8411
2.8207
2.8092
2.7052
2.1526
2.1350
1.6689
1.6501
1.6104
1.5923
1.5750
1.4025
1.3852
1.3446
1.3021
1.2801
1.2614
1.2429
1.1840
1.1104
1.0955
4.19
6.26
1.63
0.83
1.06
2.06
2.09
0.92
3.39
1.35
1.22
2.00
4.03
16.47
f1 (ppm)

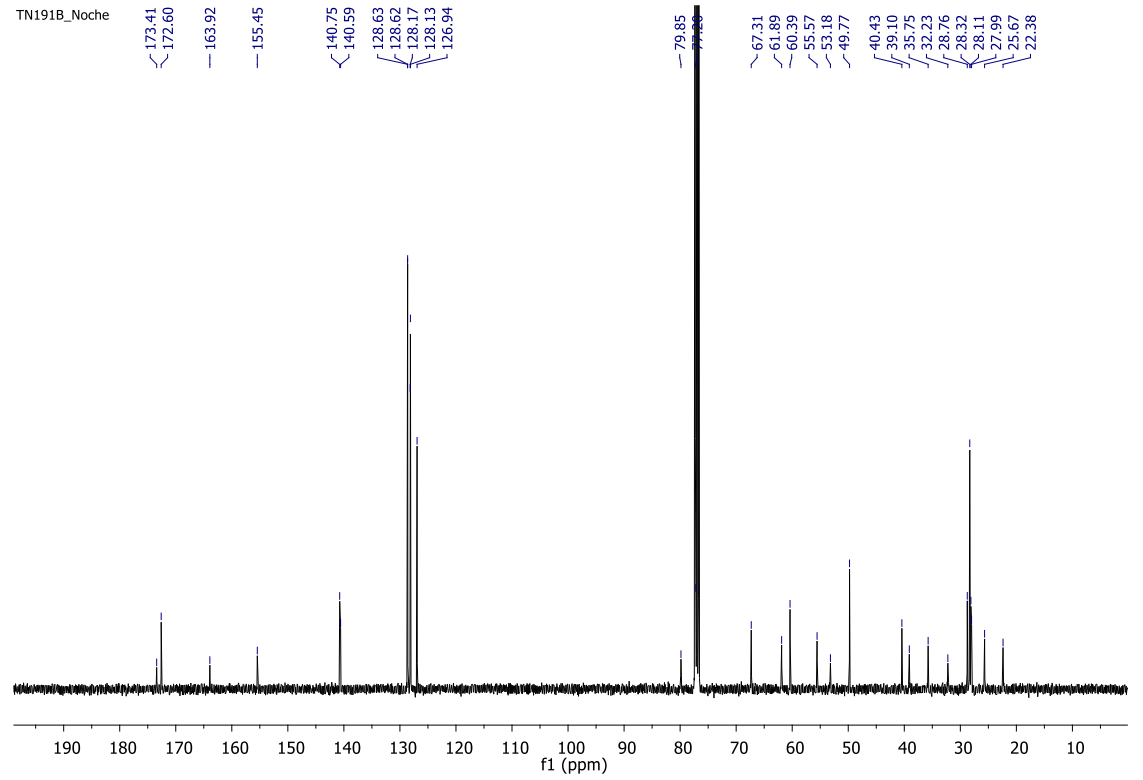
TN191B_Noche
173.41
172.60
163.92
155.45
140.75
140.59
128.63
128.62
128.17
128.13
126.94
79.85
67.31
61.89
60.39
55.57
53.18
49.77
40.43
39.10
35.75
32.23
28.76
28.32
28.11
27.99
25.67
22.38
f1 (ppm)

HSQC ($CDCl_3$)

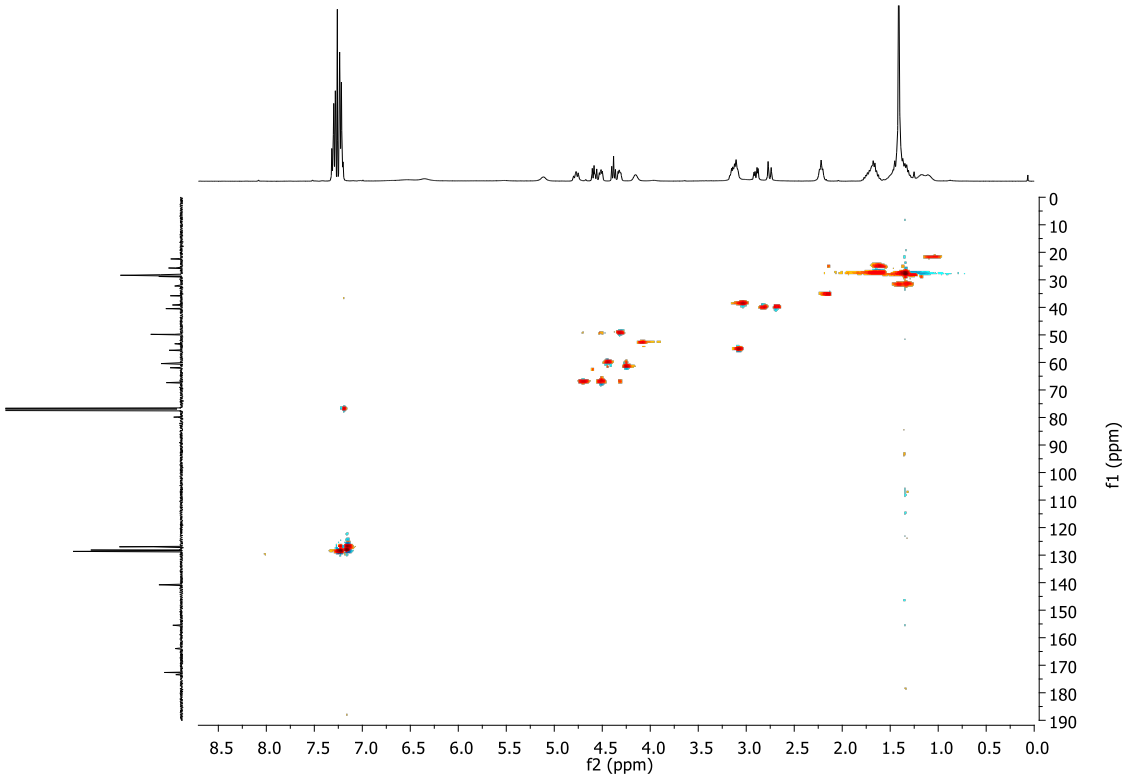
f1 (ppm)
f2 (ppm)

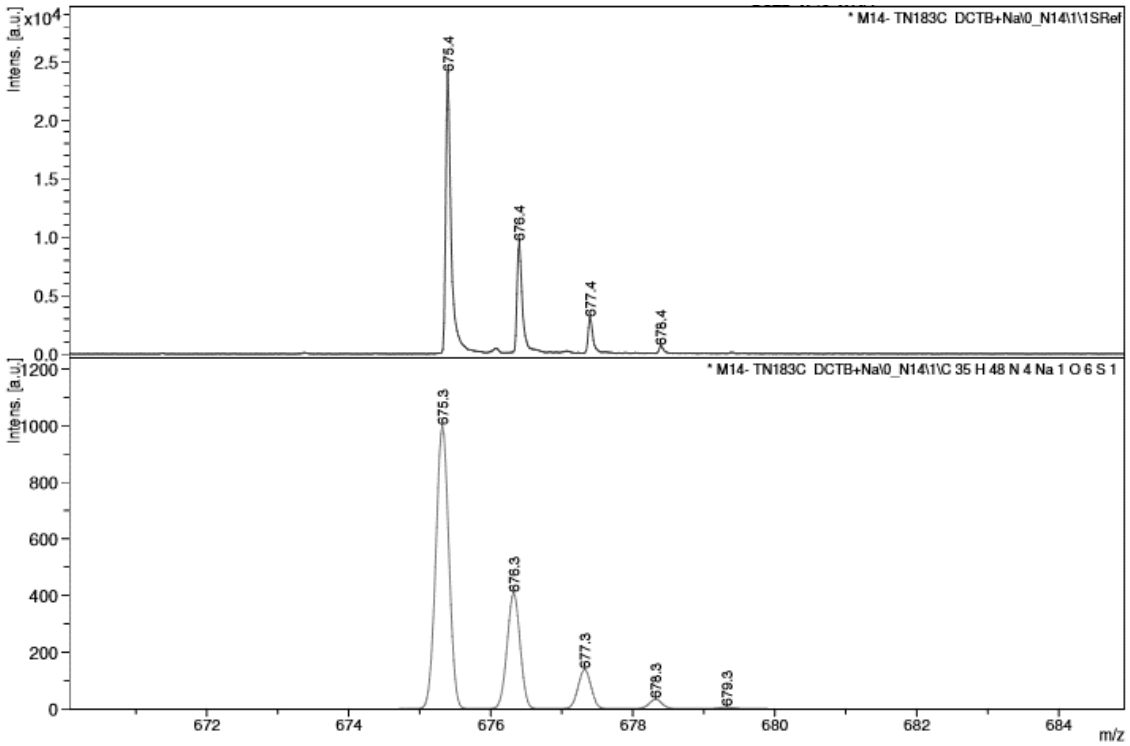
* M14- TN183C DCTB+Na\0_N14\1\1\SRef
Intens. [a.u.]
675.4
676.4
677.4
678.4
* M14- TN183C DCTB+Na\0_N14\1\1\C 35 H 48 N 4 Na 1 O 6 S 1
675.3
676.3
677.3
678.3
679.3
m/z

1-(2,2-diphenylethoxy)-1-oxo-6-(biotinylamido)hexan-2-aminium 2,2,2-trifluoroacetate

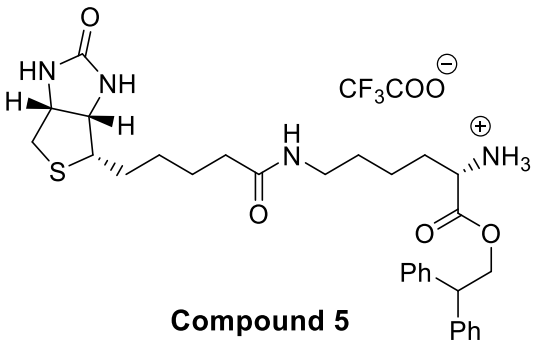

Compound 5

To a solution of compound **4** (58 mg, 0.09 mmol) in DCM (1.5 mL) TFA was added (0.1 mL) at 0ºC. The reaction was stirred at room temperature for 3h until it was completed (followed by TLC). The reaction mixture was concentrated under reduced pressure, then DCM was added and the organic layer was washed with aqueous $NaHCO_3$, further washed with brine, dried over Na_2SO_4 and concentrated under reduced pressure to give compound 5 as yellowish oil in quantitative yield. The crude material was used directly in the next reaction.

4-[(1-(2,2-diphenylethoxy)-6-(biotinylamino)-1-oxohexan-2-yl)amino]-4-oxobut-2-enoic acid

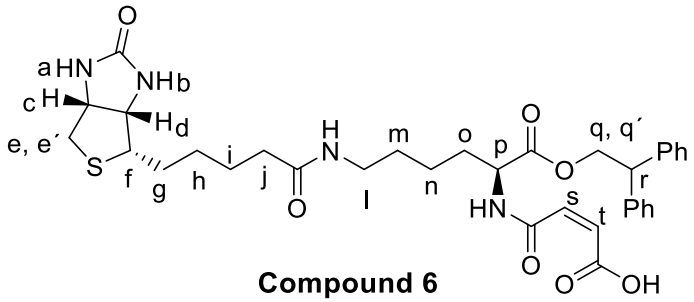

Compound 6

A solution of compound **5** (49 mg, 0.09 mmol) and Et_3N (12 μL, 0.093 mmol) in anhydrous THF (1 mL), was cooled to 0ºC, then maleic anhydride (9 mg, 0.093 mmol) dissolved in THF (0.4 mL) was added dropwise under nitrogen atmosphere. The solution was allowed to warm up to room temperature and stirred overnight. The solvent was then removed under reduced pressure and the crude material was purified by flash chromatography (using a gradient elution, starting DCM/MeOH 9:1 and then DCM/MeOH/NH_3 4:1:0.01), to furnish a yellow oil (59 mg 90% yield). ^{1}H NMR ([D6]dimethyl sulfoxide): δ = 11.09 (br s, 1H, OH), 7.91 (m, 1H, NH), 7.30 (m, 8 H, , Ar-H), 7.21 (m, 2 H, , Ar-H), 6.45 (br s, 1 H, H_a), 6.35 (br s, 1 H, H_b), 6.19 (d, J = 13.0 Hz, 1H, H_t), 5.84 (d, J = 12.8 Hz, 1H, H_s), 4.73 (dd, *J* = 7.9, 10.8 Hz, 1 H, H_q or $H_{q'}$), 4.53 (dd, *J* = 7.2, 10.9 Hz, 1 H, $H_{q'}$ or H_q), 4.36 (t, J = 7.6 Hz, 1H, H_r), 4.29 (m, 1 H, H_c), 4.10 (m, 2 H, H_d,

H_p), 3.08 (m, 1 H, H_f), 2.92 (m, 2 H, H_l), 2.81 (dd, J = 4.7, 12.9 Hz, 1 H, H_e or $H_{e'}$), 2.56 (d, J = 12.8 Hz, 1 H, $H_{e'}$ or H_e), 2.07 (t, J = 6.8 Hz, 2 H, H_j), 1.44 (m, 12 H, H_g, H_i, H_h, H_n, H_m, H_o); ^{13}C NMR ([D6]dimethyl sulfoxide): δ = 172.0, 171.7, 167.2, 165.3, 162.7, 141.3, 141.2, 136.2, 128.5 (2C), 128.5 (2C), 128.2, 128.0 (4C), 126.7 (2C), 66.3, 61.1, 59.2, 55.4, 52.3, 49.3, 39.9, 37.7, 35.2, 30.2, 28.6, 28.2, 28.0, 25.4, 22.2 ppm. MS m/z: calculated for $C_{34}H_{42}N_4O_7S$ $[M+H]^+$ 650.8 found FAB 651.3.

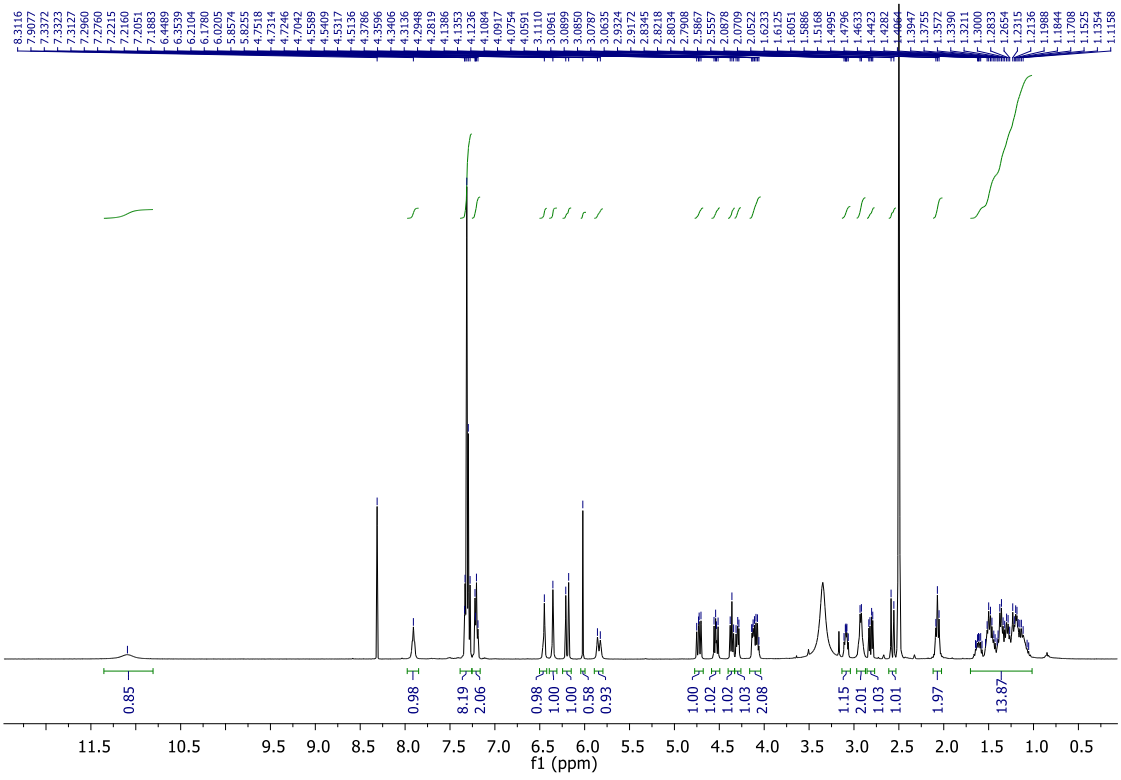

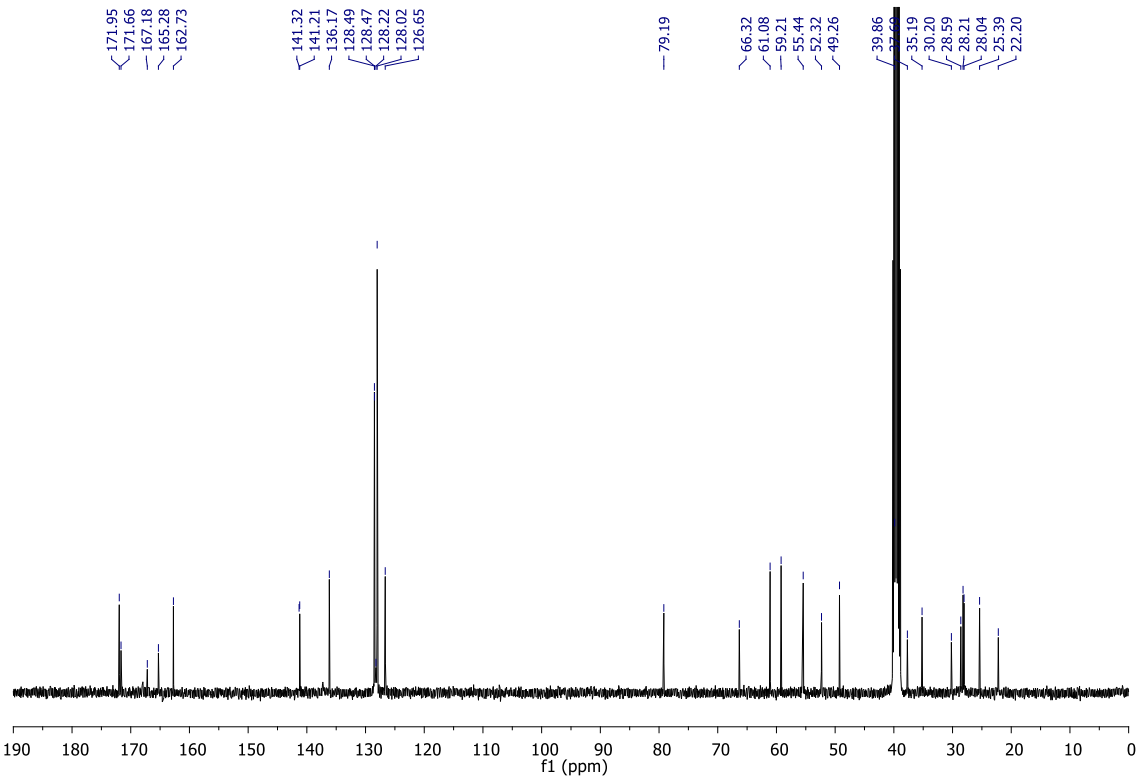

COSY ([D6]dimethyl sulfoxide)

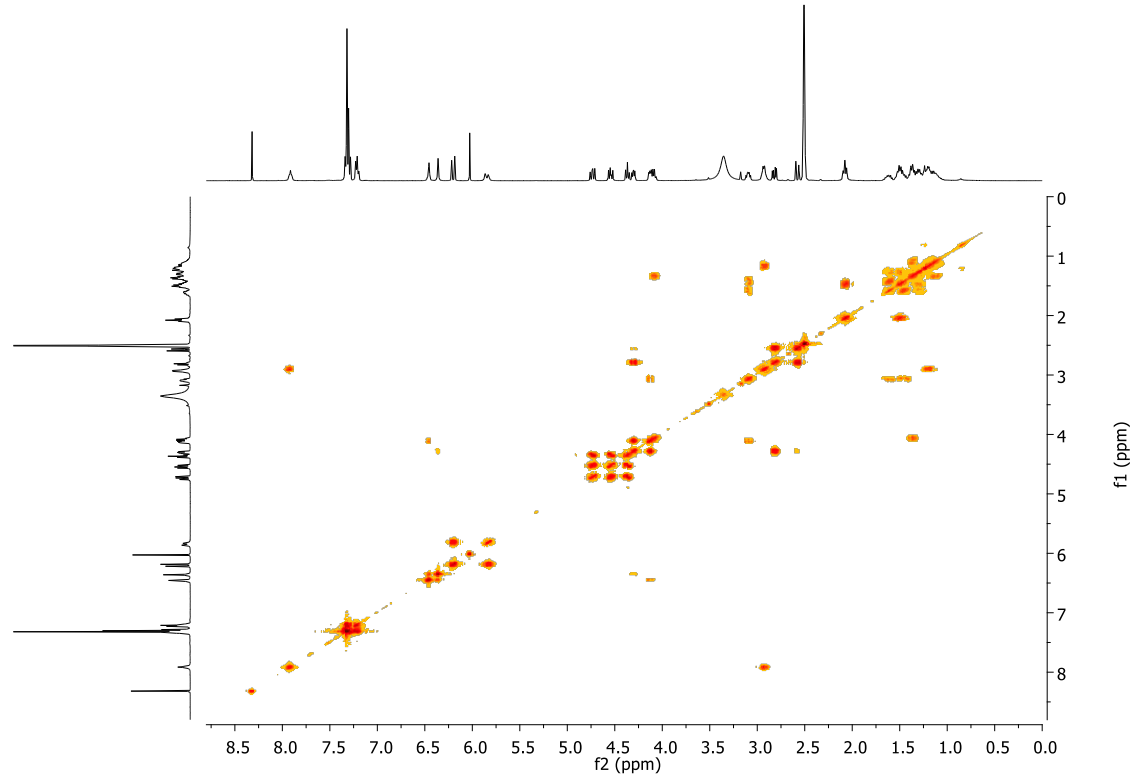

HSQC ([D6]dimethyl sulfoxide)

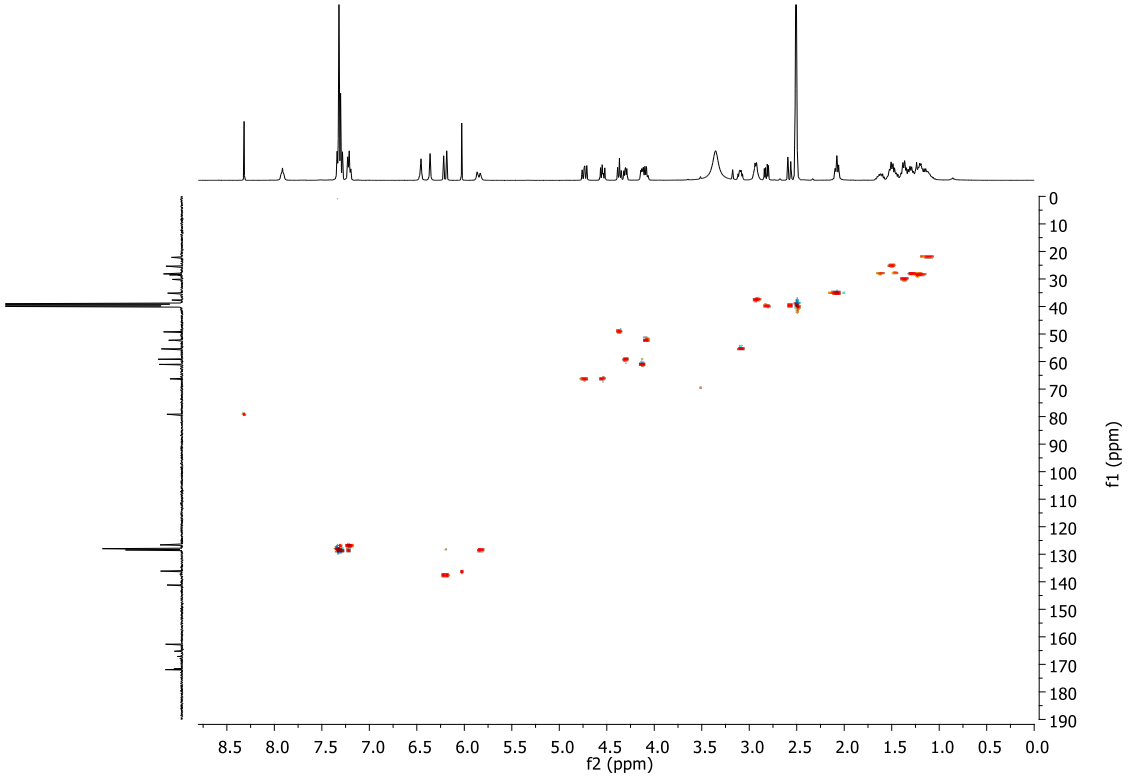

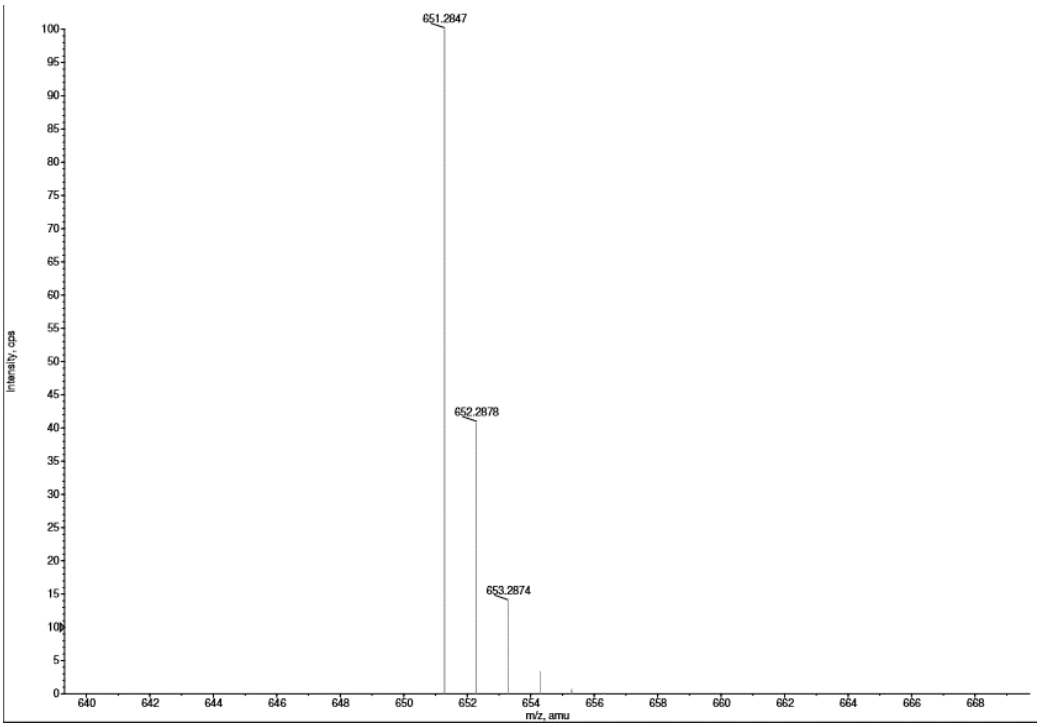

2,2-Diphenylethyl succinic acid mono ester

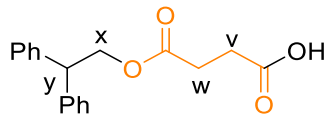

Compound 7

To a stirred solution of 2,2,-diphenylethanol (1 g, 5.26 mmol) in DCM (53mL) was added one drop of Et_3N and a solution of succinic anhydride (584 mg, 5.83 mmol) in 15 mL DCM, added slowly over 30 min. The reaction mixture was stirred overnight. Once the reaction was completed (follow by TLC), the solvent was removed under reduced pressure and the crude material was purified by column chromatography, eluent: Hexane/AcOEt 2:1, to afford 1.2 g of compound **7** as a white solid (76%). ^{1}H NMR ($CDCl_3$): δ = 7.28 (m, 4H, , Ar-H), 7.21 (m, 6H, Ar-H), 4.65 (d, J = 7.6 Hz, 2H, H_x), 4.36 (t, J = 7.6 Hz, 1H, H_y), 2.55 (m, 4 H, H_v, H_w) ppm.

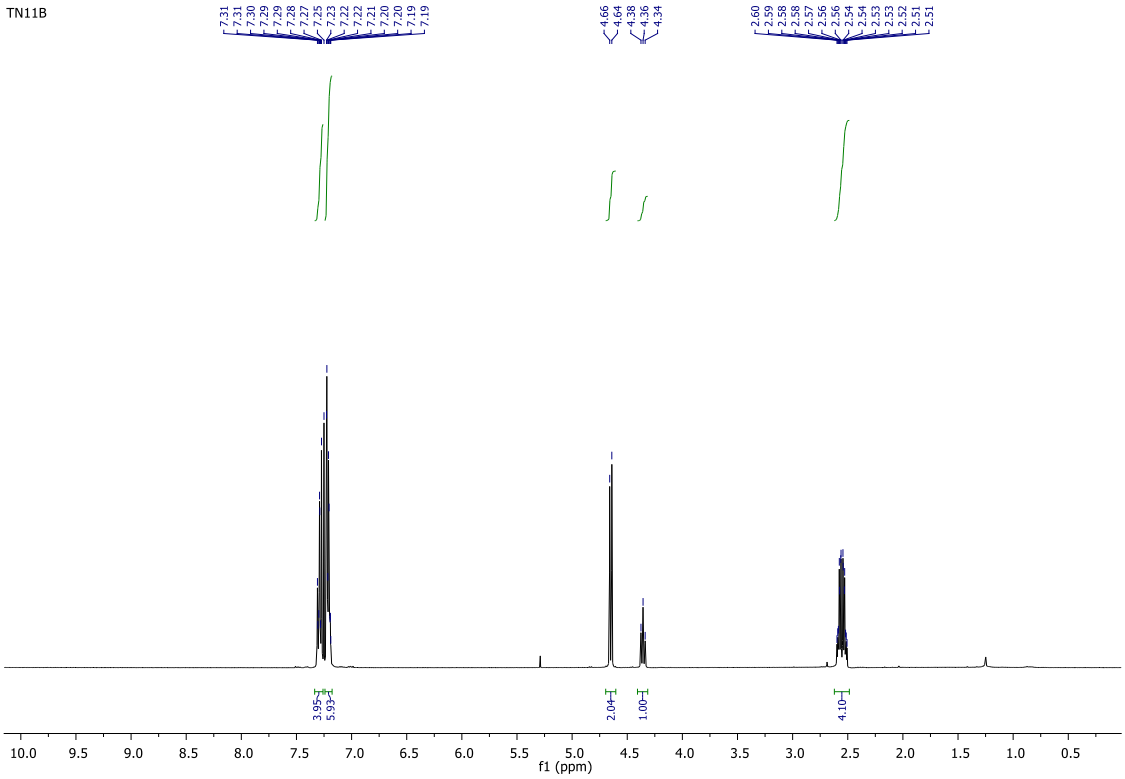

tert-Butyl (2-(2-(2-aminoethyl) hexacosaethylenoxy)ethyl carbamate

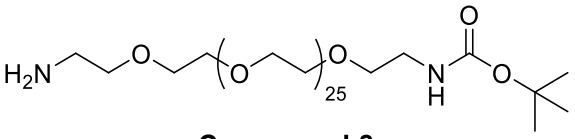

Compound 8

The reaction was carried out under anhydrous conditions. To 490mg (0.4 mmol) *O,O´*-bis (2-aminoethyl) hexacosaethylene glycol (EG26) in DCM at 0ºC was added di-tert-butyl dicarbonate (44mg, 0.2 mmol). The solution was stirred overnight, then the solvent was removed in vacuo and the crude material purified via column chromatography using a gradient elution, starting with $CHCl_3$/MeOH 10:1 to 4:1 and finally 1:1, to give a yellowish oil, 165 mg, 61%. ^{1}H NMR ($CDCl_3$): δ = 7.91 (br s 3H, 3NH), 3.92 (m, 2H), 3.63 (m, 106H, EG26-H), 3.52 (t, *J* = 5.1, 2H), 3.29 (t, *J* = 5.2, 2H), 3.17 (m, 2H), 1.43 (s, 9H, Boc-H); ^{13}C NMR ($CDCl_3$): δ = 154.9, 79.0, 70.5 (51C), 70.3, 70.0, 69.8, 40.4, 29.7, 40.4 (3C) ppm. MS m/z: calculated for $C_{61}H_{124}N_2O_{29}$ $[M+Na]^+$ 1371.8 found MALDI-TOF 1371.8.

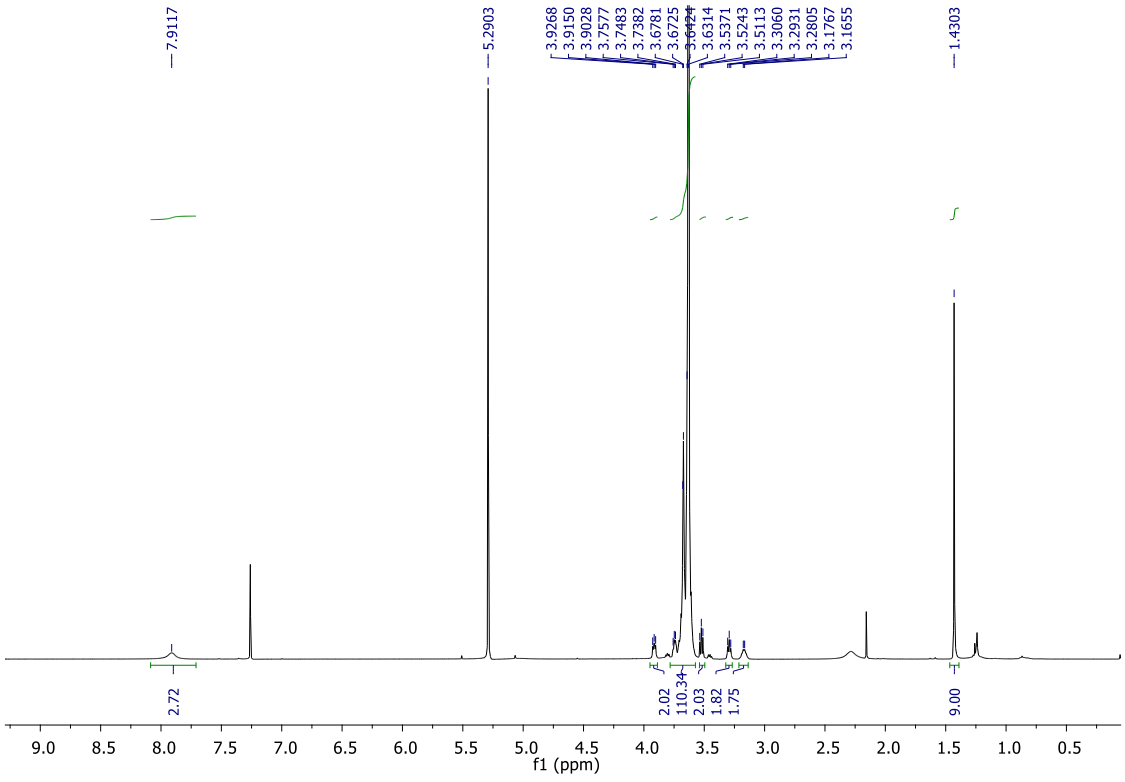

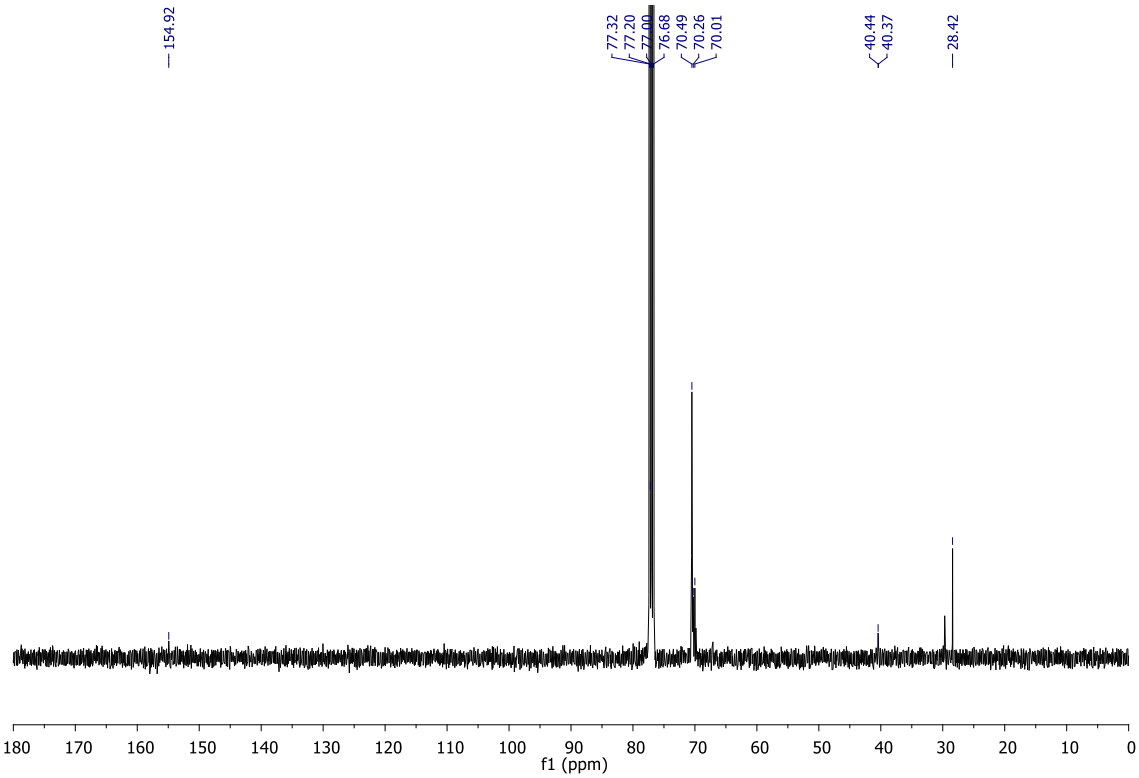
154.92
77.32
77.20
77.00
76.68
70.49
70.26
70.01
40.44
40.37
28.42
180 170 160 150 140 130 120 110 100 90 80 70 60 50 40 30 20 10 0
f1 (ppm)

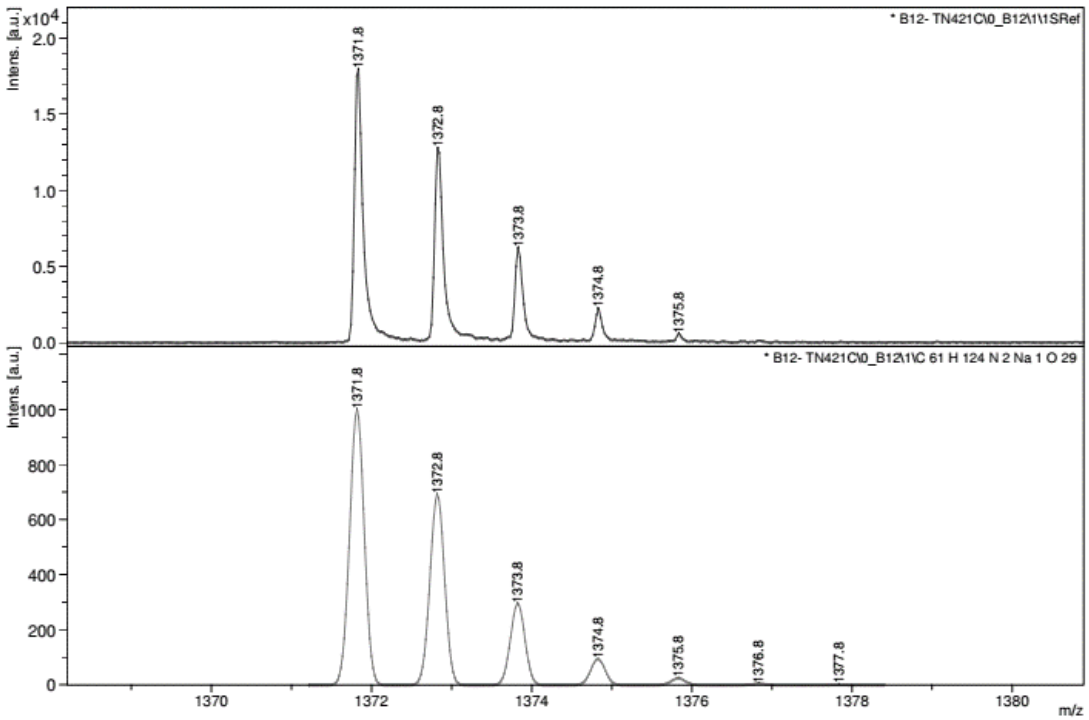
Intens. [a.u.]
x10^4
2.0
1.5
1.0
0.5
0.0
* B12- TN421C\0_B12\1\1SRef
1371.8
1372.8
1373.8
1374.8
1375.8
Intens. [a.u.]
1000
800
600
400
200
0
* B12- TN421C\0_B12\1\C 61 H 124 N 2 Na 1 O 29
1371.8
1372.8
1373.8
1374.8
1375.8
1376.8
1377.8
1370
1372
1374
1376
1378
1380
m/z

2,2-diphenylethyl 2,2-dimethyl-4,18-dioxo-3,8,11,14-tetraoxa-5,17-diazahenicosan-21-oate

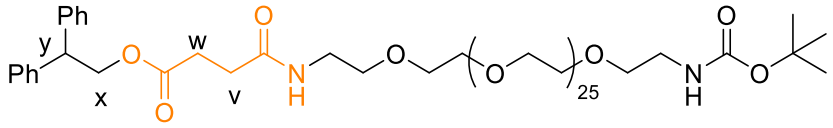

Compound 9

40 mg (0.13 mmol) of compound **7** was dissolved in DCM (2 mL) and the solution was cooled down to 0ºC. Then EDCI (38 mg, 0.2 mmol) and DMAP (24 mg, 0.2 mmol) were added at 0ºC and the reaction mixture was allowed to stir at room temperature for 30 min. A solution of compound **8** (165 mg, 0.12 mmol), in DCM (1.5 mL) was added to the activated acid. The reaction mixture was stirred for 24h, concentrated under reduced pressure and then diluted with DCM and washed with 1M HCl, with $NaHCO_3$ (sat. aq.). The organic layer was further washed with brine (sat.), dried over Na_2SO_4 and concentrated under reduced pressure. The crude material was purified by column chromatography using $CHCl_3$/MeOH 15:1 as eluent, to give compound **9** as a colorless oil, 180mg, 92%. ^{1}H NMR ($CDCl_3$): δ = 7.28 (m, 4H, Ar-H), 7.21 (m, 6H, Ar-H), 6.23 (br s, 1H, NH), 5.03 (br s, 1H, NH), 4.62 (d, *J* = 7.6 Hz, 2H, H_x), 4.35 (t, *J* = 7.6 Hz, 1H, H_y), 3.81 (m, 1H), 3.63 (m, 103H, EG26-H), 3.53 (m, 4H), 3.40 (m, 2H), 3.30 (m, 2H), 2.57 (t, 2H, *J* = 7.2 Hz, H_w), 2.37 (t, 2H, *J* = 7.0 Hz, H_v),1.43 (s, 9H, Boc-H); ^{13}C NMR ($CDCl_3$): δ = 172.7, 171.5, 156.0, 141.1 (2C), 128.5 (4C), 128.2 (4C), 126.8 (2C), 79.2, 70.6 (51C), 70.2, 70.2, 69.7, 66.8, 49.8, 40.5, 39.4, 30.6, 29.7, 28.4 (3C) ppm. MS m/z: calculated for $C_{79}H_{140}N_2O_{32}$ $[M+Na]^+$ 1651.9 found MALDI-TOF 1651.9.

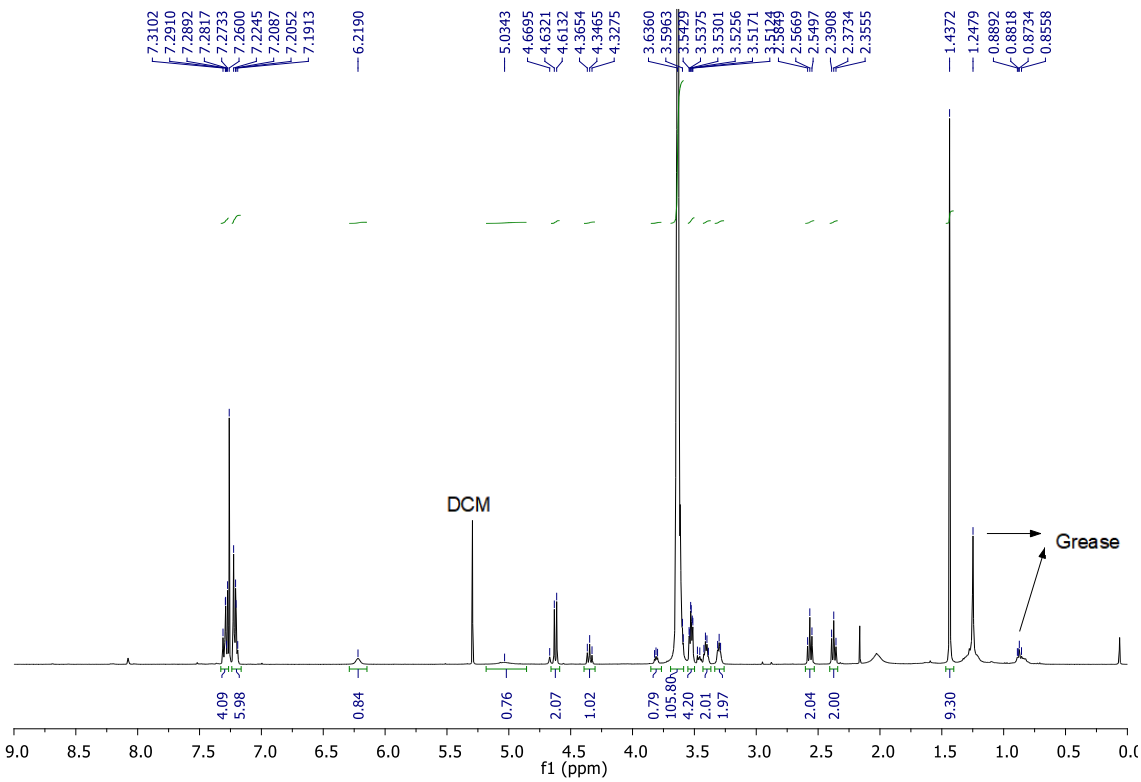
DCM
Grease
f1 (ppm)

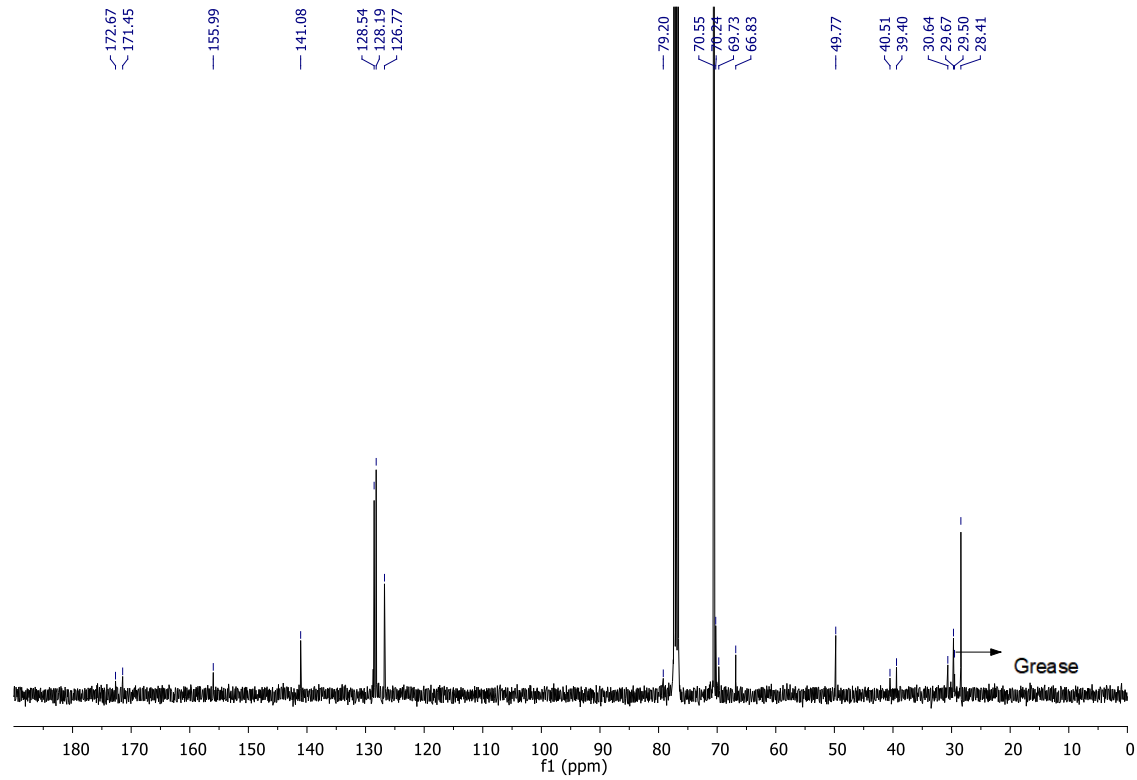
Grease
f1 (ppm)

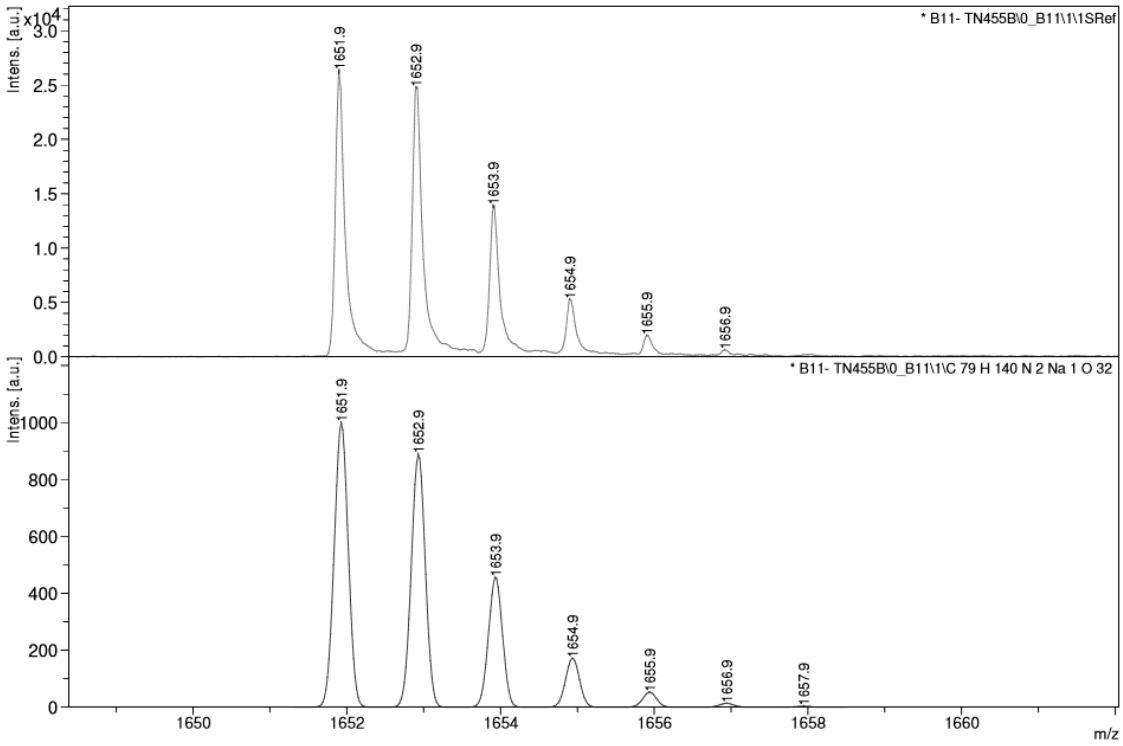

Compound 10 was synthetized following the same procedure described for compound 5.

(Z/E 55/45)-Thread

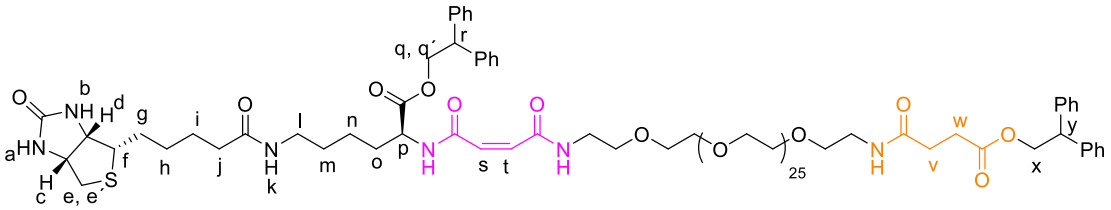

Compound 11

Compound **6** (85 mg, 0.13 mmol) was dissolved in DCM (3 mL) and the solution was cooled to 0ºC, EDCI (23 mg, 0.19 mmol), DMAP (37 mg, 0.19 mmol) were added at 0ºC. The reaction mixture was allowed to stir at room temperature for 30 min, and then a solution of compound **10** (180 mg, 0.12 mmol) in DCM (7.7 mL) was added to the activated acid. The reaction mixture was stirred overnight, concentrated under reduced pressure and then diluted with DCM. The organic layer was washed with 1M HCl, with $NaHCO_3$ (sat. aq.), then further washed with brine (sat. aq.), dried over Na_2SO_4 and concentrated under reduced pressure. The crude material was purified by column chromatography (gradient elution: DCM/MeOH 30:1 to 9:1) to furnish the

desired product as a colorless oil, 166mg, 0.077 mmol (64%).[1]H NMR ([D6]dimethyl sulfoxide): δ = 8.65 (d, *J* = 7.2 Hz, 1H, NH), 8.50 (t, *J* = 5.6 Hz, 1H, NH), 7.86 (t, *J* = 5,5 Hz, 1H, NH), 7.70 (t, *J* = 5,5 Hz, 1H, NH), 7.27 (m, 16 H, Ar-H), 7.21 (m, 4 H, Ar-H), 6.87 (d, J = 15.5 Hz, 0.4 H, H_r or H_s of *E*-isomer), 6.82 (d, J = 15.5 Hz, 0.4 H, H_r or H_s of *E*-isomer), 6.40 (br s, 1 H, H_a), 6.34 (br s, 0.5 H, H_b), 6.21 (d, *J* = 13.1 Hz, 0.5 H, H_r or H_s of *Z*-isomer), 6.08 (d, *J* = 13.1 Hz, 1H, H_s or H_t of *Z*-isomer), 4.72 (dd, *J* = 8.1, 10.9 Hz, 1 H, H_q or $H_{q'}$), 4.55 (m, 3H, $H_{q'}$ or H_q, H_x), 4.33 (m, 3H, H_c, H_y, H_r), 4.12 (m, 2H, H_d, H_p), 3.68 (m, 1H, EG26-H), 3.50 (m, 107H, EG26-H), 3.37 (t, *J* = 6.0 Hz, 2H, EG26-H), 3.17 (dd, *J* = 5.8, 11.5 Hz, 2H, EG26-H), 3.08 (m, 1H, H_f), 2.91 (m, 2 H, H_l), 2.81 (dd, *J* = 4.7, 12.9 Hz, 1 H, H_e or $H_{e'}$), 2.54 (d, *J* = 12.8 Hz, 1 H, $H_{e'}$ or H_e), 2.37 (t, *J* = 6.9 Hz, 2 H, H_w), 2.27 (t, *J* = 6.6 Hz, 2 H, H_v), 2.04 (t, *J* = 6.8 Hz, 2 H, H_j), 1.44 (m, 12 H, H_g, H_i, H_h, H_n, H_m, H_o) (400 MHz, DMSO) ppm. MS m/z: calculated for $C_{108}H_{172}N_6O_{36}S$ $[M+Na]^+$ 2185.1 found MALDI-TOF 2185.1.

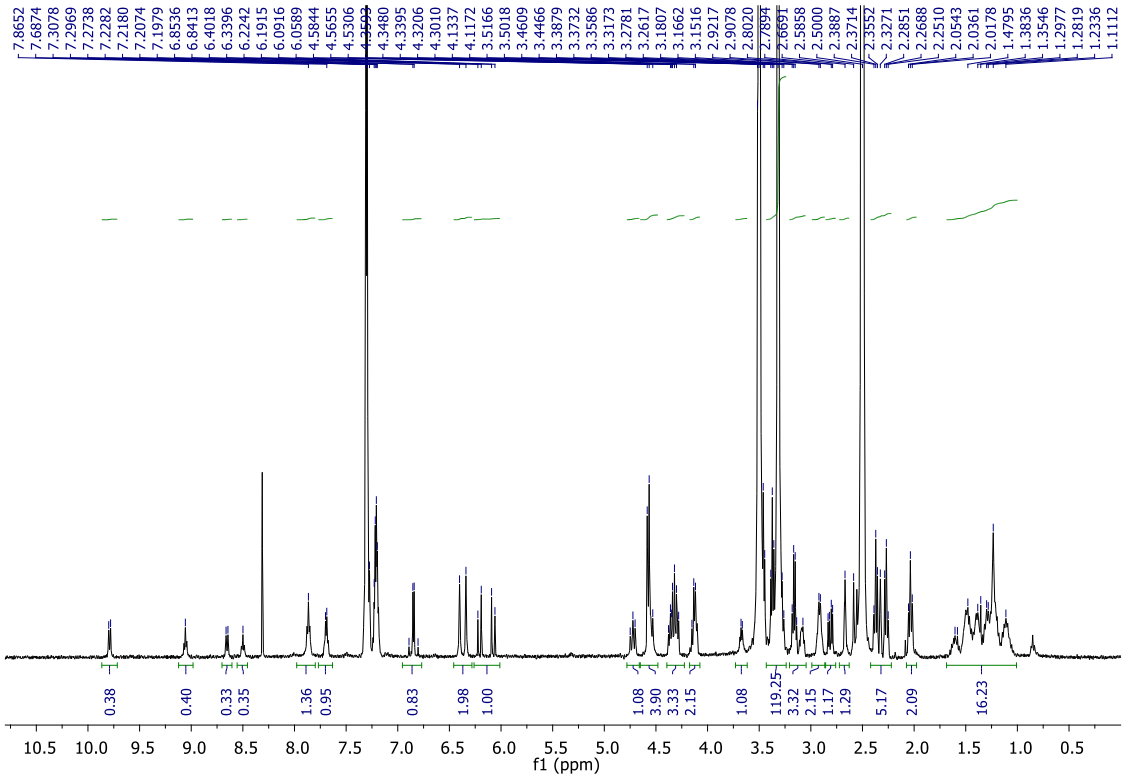

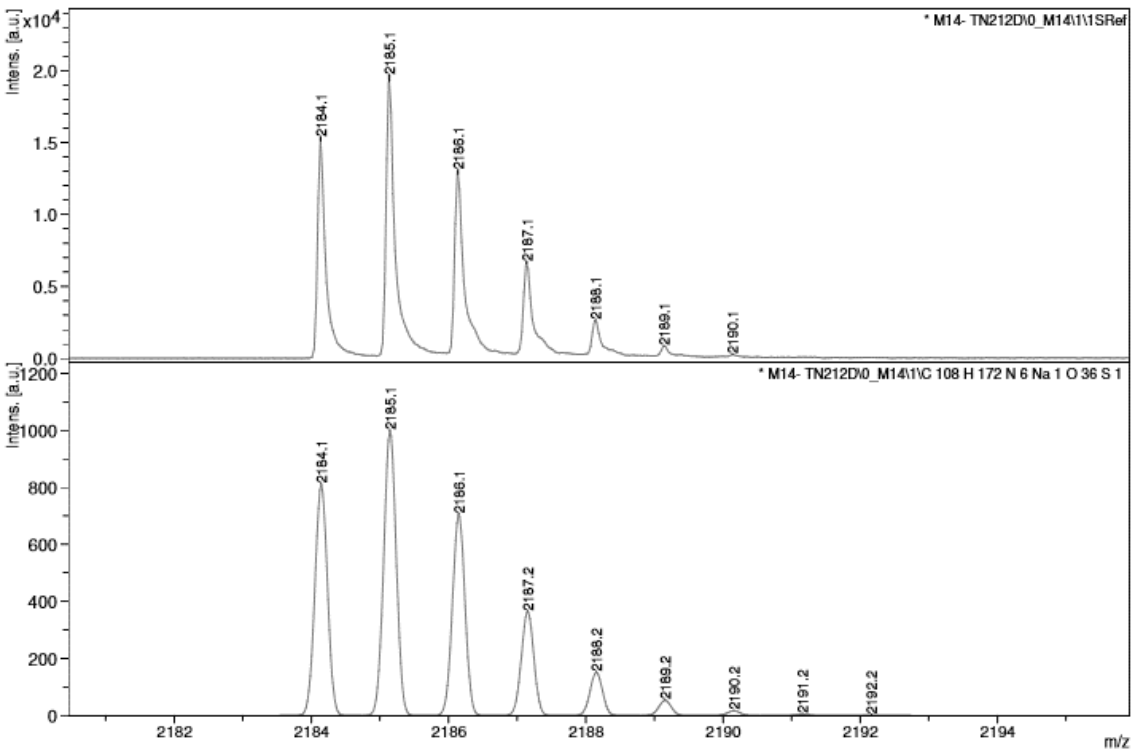

(E)-Thread

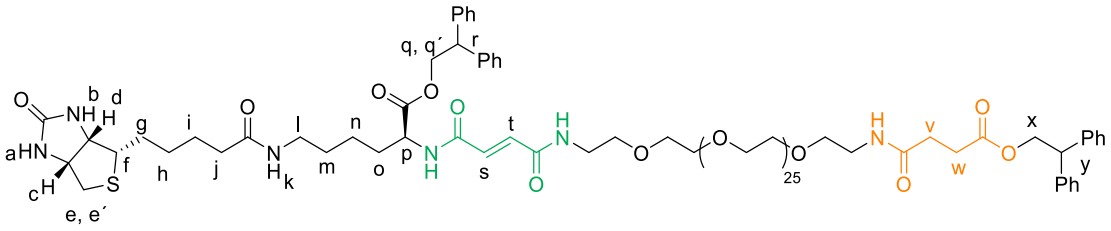

Compound 12

A solution of compound **11** (115 mg, 0.052mmol) and piperidine (4 µg, 0.006 mmol) in DCM (3 mL) was stirred for 48 h. Then DCM was added and the organic layer was washed twice with 1M HCl. The organic layer was concentrated under reduced pressure to furnish compound **12** as yellowish oil (112 mg, 97%). ^{1}H NMR ([D6]dimethyl sulfoxide): δ = 8.65 (d, *J* = 7.2 Hz, 1H, NH), 8.50 (t, *J* = 5.6 Hz, 1H, NH), 7.86 (t, *J* = 5,5 Hz, 1H, NH), 7.70 (t, *J* = 5,5 Hz, 1H, NH), 7.27 (m, 16 H, Ar-H), 7.21 (m, 4 H, Ar-H), 6.87 (d, J = 15.5 Hz, 1H, H_s or H_t), 6.82 (d, J = 15.5 Hz, 1H, H_s or H_t), 6.40 (br s, 1 H, H_a), 6.34 (br s, 1 H, H_b), 4.72 (dd, *J* = 8.1, 10.9 Hz, 1 H, H_p or $H_{p'}$), 4.55 (m, 3H, $H_{q'}$ or H_q, H_x), 4.33 (m, 3H, H_c, H_y, H_r), 4.12 (m, 2H, H_d, H_p), 3.68 (m, 1H, EG26-H), 3.50 (m, 107H, EG26-H), 3.37 (t, *J* = 6.0 Hz, 2H, EG26-H), 3.17 (dd, *J* = 5.8, 11.5 Hz, 2H, EG26-H), 3.08 (m, 1H, H_f), 2.91 (m, 2 H, H_l), 2.81 (dd, *J* = 4.7, 12.9 Hz, 1 H, H_e or $H_{e'}$), 2.54 (d, *J* = 12.8 Hz, 1 H, $H_{e'}$ or H_e), 2.37 (t, *J* = 6.9 Hz, 2 H, H_w), 2.27 (t, *J* = 6.6 Hz, 2 H, H_v),

2.04 (t, J = 6.8 Hz, 2 H, H_j), 1.44 (m, 12 H, H_g, H_i, H_h, H_n, H_m, H_o); ^{13}C NMR ([D6]dimethyl sulfoxide): δ = 173.4, 172.7, 171.9, 171.2, 165.4, 164.6, 163.6, 141.1 (2C), 140.8, 140.8, 140.6, 140.5, 133.4, 132.4, 129.7, 128.6 (2C), 128.6 (2C), 128.5 (4C), 128.3, 128.2 (4C), 128.1 (2C), 126.9 (2C), 126.7(2C), 70.5 (50C), 70.5, 70.2, 69.8, 69.6, 67.3, 66.7, 55.5, 52.3, 49.7, 49.7, 40.4, 39.6, 39.3, 38.3, 35.7, 30.9, 30.7, 29.6, 29.4, 28.7, 28.0, 25.5, 22.6, 21.9 ppm. MS m/z: calculated for $C_{108}H_{172}N_6O_{36}S$ $[M+Na]^+$ 2184.0 found FAB 2184.1.

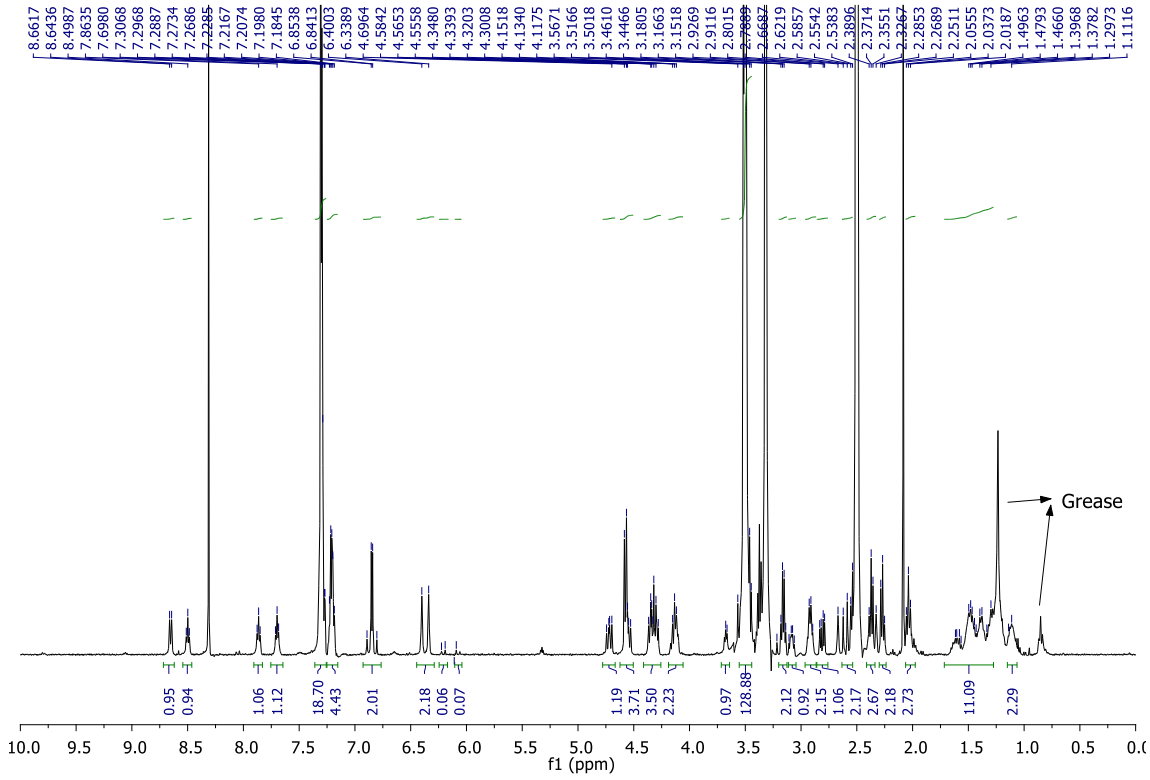

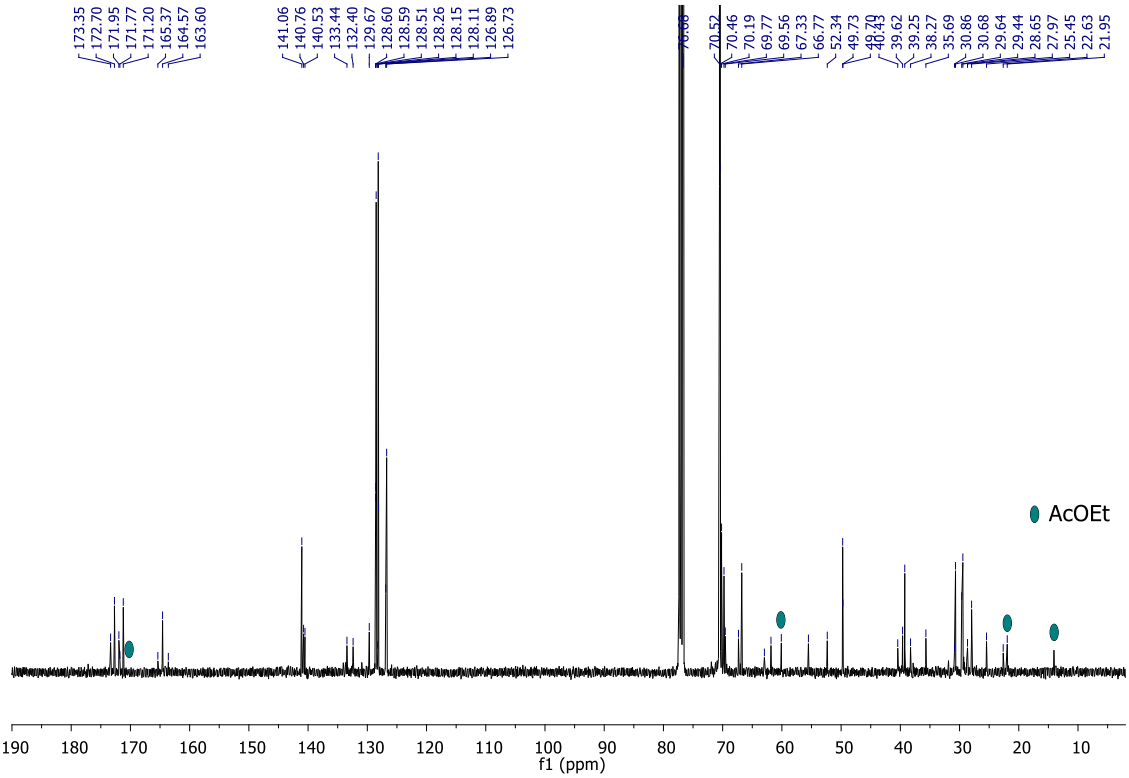
173.35
172.70
171.95
171.77
171.20
165.37
164.57
163.60
141.06
140.76
140.53
133.44
132.40
129.67
128.60
128.59
128.51
128.26
128.15
128.11
126.89
126.73
78.68
70.52
70.46
70.19
69.77
69.56
67.33
66.77
52.34
49.73
48.70
40.43
39.62
39.25
38.27
35.69
30.86
30.68
29.64
29.44
28.65
27.97
25.45
22.63
21.95
AcOEt
190
180
170
160
150
140
130
120
110
100
90
80
70
60
50
40
30
20
10
f1 (ppm)

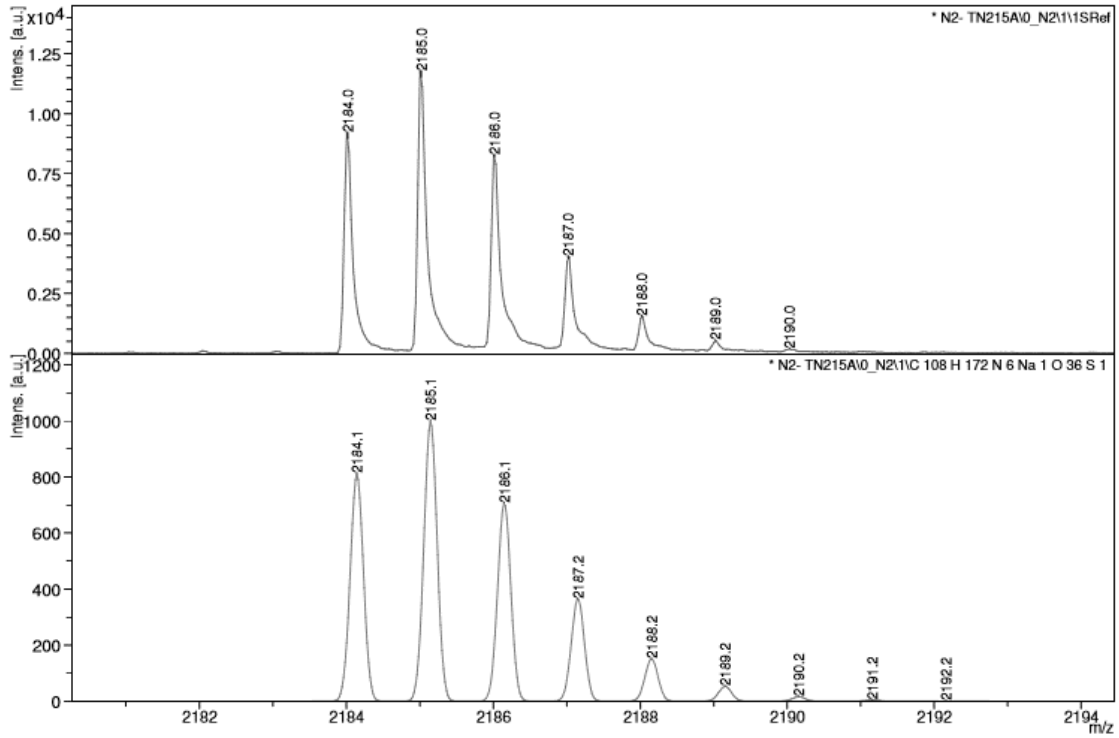
Intens. [a.u.]
x10^4
1.25
1.00
0.75
0.50
0.25
0.00
* N2- TN215A\0_N2\1\1SRef
2184.0
2185.0
2186.0
2187.0
2188.0
2189.0
2190.0
Intens. [a.u.]
1200
1000
800
600
400
200
0
* N2- TN215A\0_N2\1\C 108 H 172 N 6 Na 1 O 36 S 1
2184.1
2185.1
2186.1
2187.2
2188.2
2189.2
2190.2
2191.2
2192.2
2182
2184
2186
2188
2190
2192
2194
m/z

5-azidoisophthaloyl dichloride

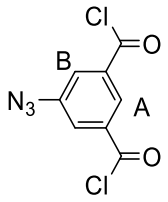

Compound 13

Step i) 5-aminoisophalic acid (2.5 g, 27.6 mmol) was placed in a flash with water (39 mL), 3 mL of 12M HCl was added dropwise. The mixture was cooled in a ice bath at 0ºC. NaNO2 was dissolved in water and added dropwise to the mixture, which was stirred for 30 min. Then, NaN_3 dissolved in water was added dropwise to the mixture. A yellow solid was formed and gas evolution was observed, making it difficult to keep stirring. The mixture was stirred until gas evolution was no longer detected. The product was then filtered, washed with distilled water and dried under vacuum (3.4g, 60%). ^{1}H NMR ([D6]dimethyl sulfoxide): δ = 13.49 (br s, 2H, OH), 8.22 (t, J = 1.4 Hz, 1H, Ar-H, H_A), 7.73 (d, J = 1.4 Hz, 1H, Ar-H, H_B) ppm. Step ii) To a stirred suspension of 5-azido-isophthalic acid (100 mg, 0.48 mmol) in DCM (2mL) two drops of anhydrous DMF and oxalyl chloride (0.15 mL, 1.95 mmol) were added. The reaction mixture was stirred until the product was totally solubilized. The solvent was removed under reduced pressure and the sample was kept 3 h under vacuum to remove oxalyl chloride. The crude product was then used directly in the next reaction step.

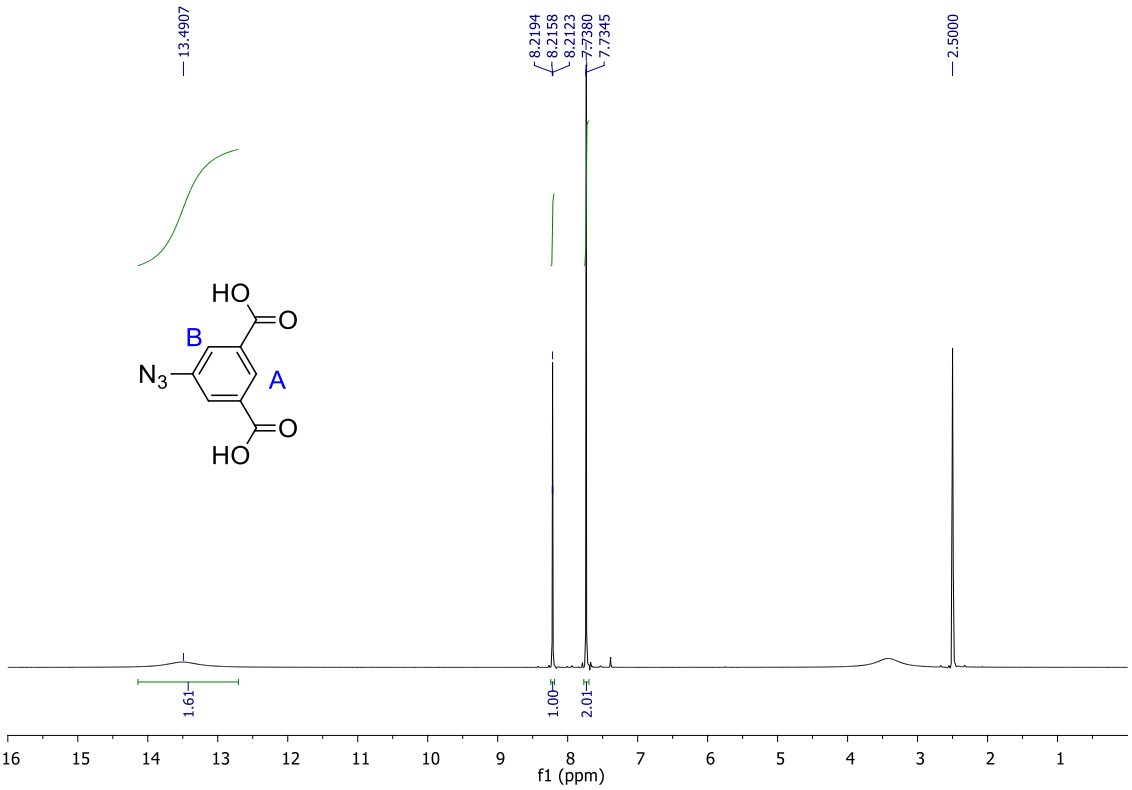
13.4907
8.2194
8.2158
8.2123
7.7380
7.7345
2.5000
HO
O
B
N3
A
O
HO
1.61
1.00
2.01
16
15
14
13
12
11
10
9
8
7
6
5
4
3
2
1
f1 (ppm)

Scheme for the synthesis of compound 14

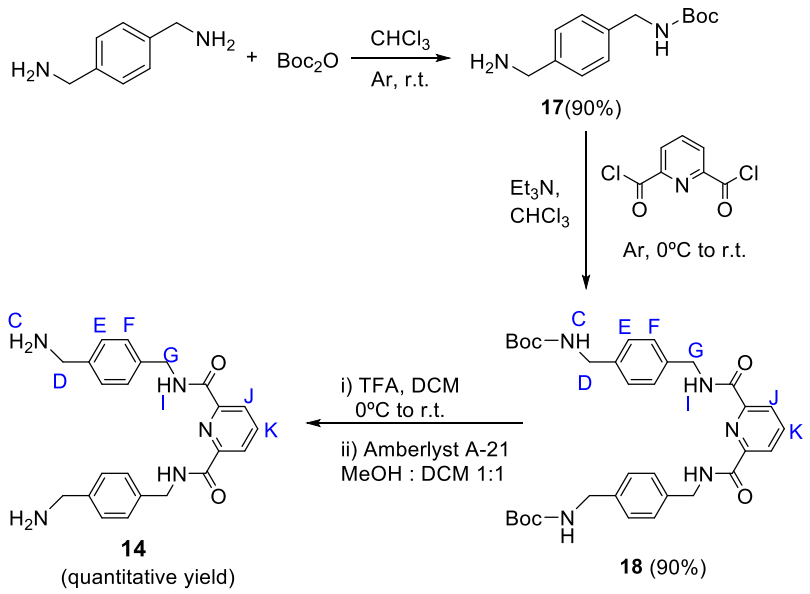

N^2,N^6-bis(4-(aminomethyl)benzyl)pyridine-2,6-dicarboxamide

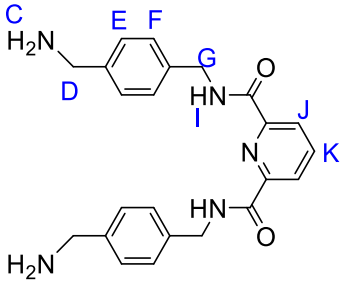

Compound 14

Step i). To a solution of *p*-xylylenediamine (515 mg, 3.78 mmol) in chloroform (60 mL) at 0 ºC, a solution of di-*tert*-butyl carbonate (413 mg, 1.89 mmol) in $CHCl_3$ (45 mL) was added dropwise over a period of 4h. The mixture was stirred at room temperature overnight under Ar. A white solid was filtered from the solution and washed with cold $CHCl_3$. The filtrate was concentrated under reduced pressure. To the remaining oil, DCM and water was added. The layers were separated and the aqueous layer was extracted with DCM (x3). The extracts were combined and dried over Na_2SO_4. The crude material was purified using a gradient elution (DCM/MeOH 15:1

to 6:1) to give compound **17** as yellowish solid (400 mg, 90%) ^{1}H NMR ($CDCl_3$): δ = 7.26 (m, 4H, Ar-H), 4.28 (m, 2H), 3.84 (s, 2H) ppm.

Step ii) 2,6-Pyridinedicarboxylic acid (234 mg, 1.4 mmol) was suspended in anhydrous DCM, the mixture was cooled to 0ºC, then oxalyl chloride was added dropwise followed by the addition of 2 drops of DMF. The reaction mixture was stirred until the product was totally solubilized. The solvent was removed and the crude solid was dried under vacuum for 2 h. The acid chloride (221 mg, 1.1 mmol) dissolved in CH_3Cl, was added dropwise to a solution of compound **14** and Et_3N in CH_3Cl. The reaction mixture was stirred overnight. The solvent was removed under reduced pressure. To the remaining oil, DCM and water were added. The layers were separated and the aqueous layer was extracted with DCM (x3). The extracts were combined and dried over Na_2SO_4. The crude material was purified using column chromatography, with a gradient elution (DCM/MeOH 15:1 to 6:1) to give compound **18** as yellowish solid (400 mg, 90%) ^{1}H NMR ($CDCl_3$): δ = 8.90 (br s, 2H, NH, H_I), 8.27 (d, *J* = 7.8 Hz, 2H, Ar-H, H_J), 7.95 (t, *J* = 7.8 Hz, 1H, Ar-H, H_K), 7.03 (m, 4H, H_F), 6.97 (m, 4H, H_E), 5.28 (br s, 2H, NH, H_C), 4.31 (br d, *J* = 5.5 Hz, 4H, H_G), 4.09 (br d, *J* = 5.9 Hz, 4H, H_D), 1.40 (s, 18H, Boc-H); ^{13}C NMR ($CDCl_3$): δ = 163.8, 156.2, 148.8, 138.7, 138.1, 137.2, 127.7, 127.2, 125.0, 79.5, 44.1, 43.0, 28.4 ppm.

Step iii) Compound **18** was dissolved in DCM, the solution was cooled to 0 ºC and TFA was added dropwise until the reaction was completed (TLC). Solvent was removed under vacuum. The crude material was dissolved in DCM/MeOH 1/1 v/v ratio and was stirred with Amberlyst A-21 resin for 1h. The solvent was removed under reduced pressure to yield compound **14** as a hygroscopic powder (quantitative yield). ^{1}H NMR ([D6]dimethyl sulfoxide): δ = 9.92 (br t, *J* = 6.4 Hz, 2H, NH, H_I), 8.22 (m, 3H, Ar-H, H_J, H_K), 7.37 (m, 4H, H_F), 7.33 (m, 4H, H_E), 4.31 (br d, *J* = 6.4 Hz, 4H, H_G), 4.09 (br s, 4H, H_D).

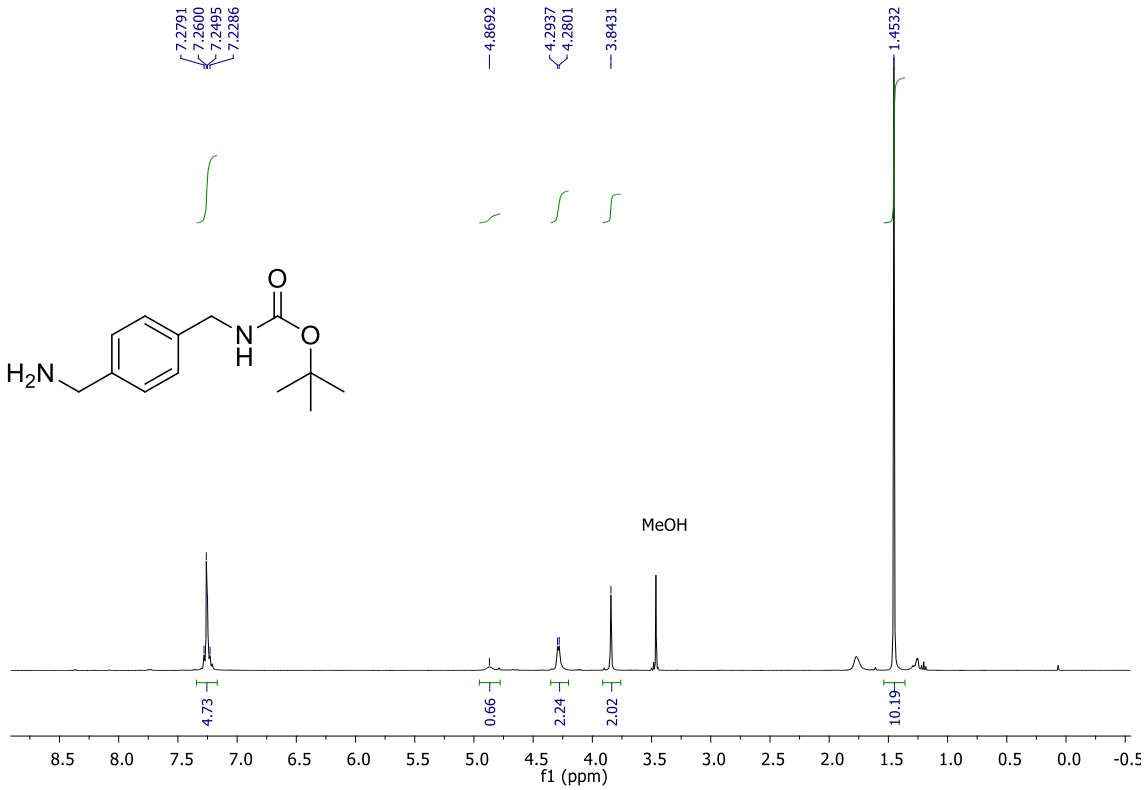
7.2791
7.2600
7.2495
7.2286
4.8692
4.2937
4.2801
3.8431
1.4532
O
N
H
O
H_2N
MeOH
4.73
0.66
2.24
2.02
10.19
f1 (ppm)

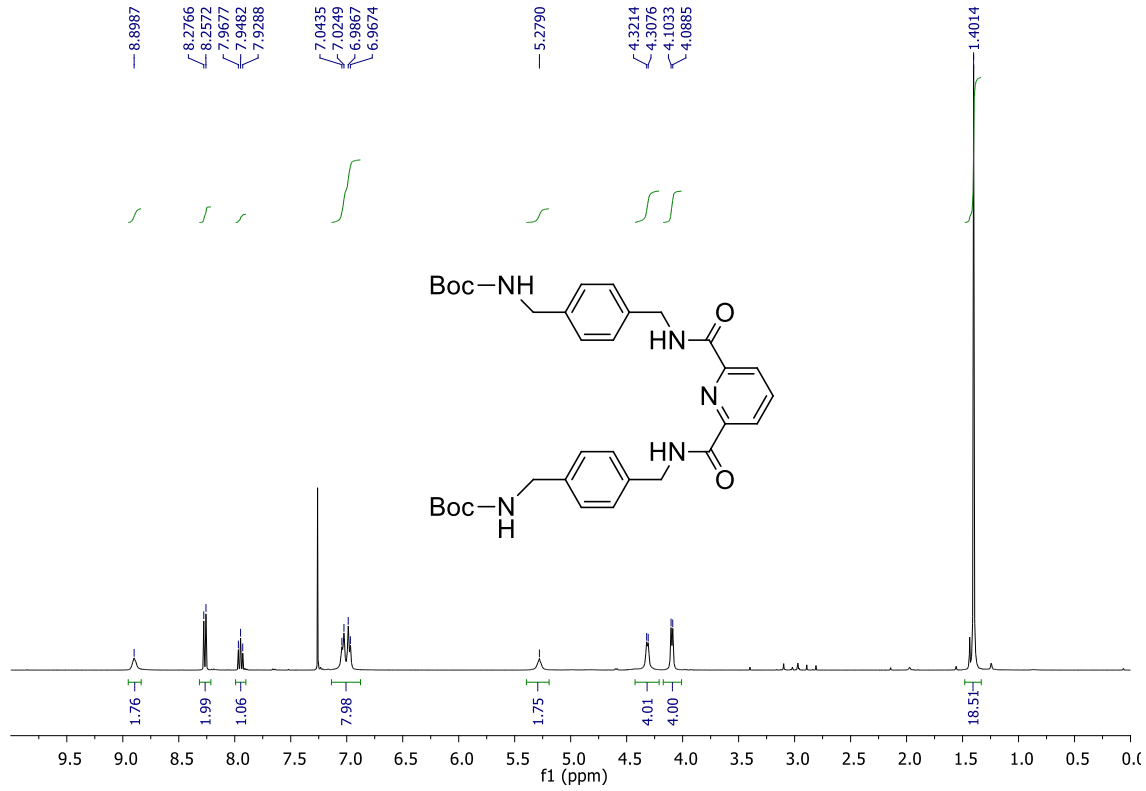
8.8987
8.2766
8.2572
7.9677
7.9482
7.9288
7.0435
7.0249
6.9867
6.9674
5.2790
4.3214
4.3076
4.1033
4.0885
1.4014
Boc—NH
HN
O
N
HN
O
Boc—N
H
1.76
1.99
1.06
7.98
1.75
4.01
4.00
18.51
f1 (ppm)

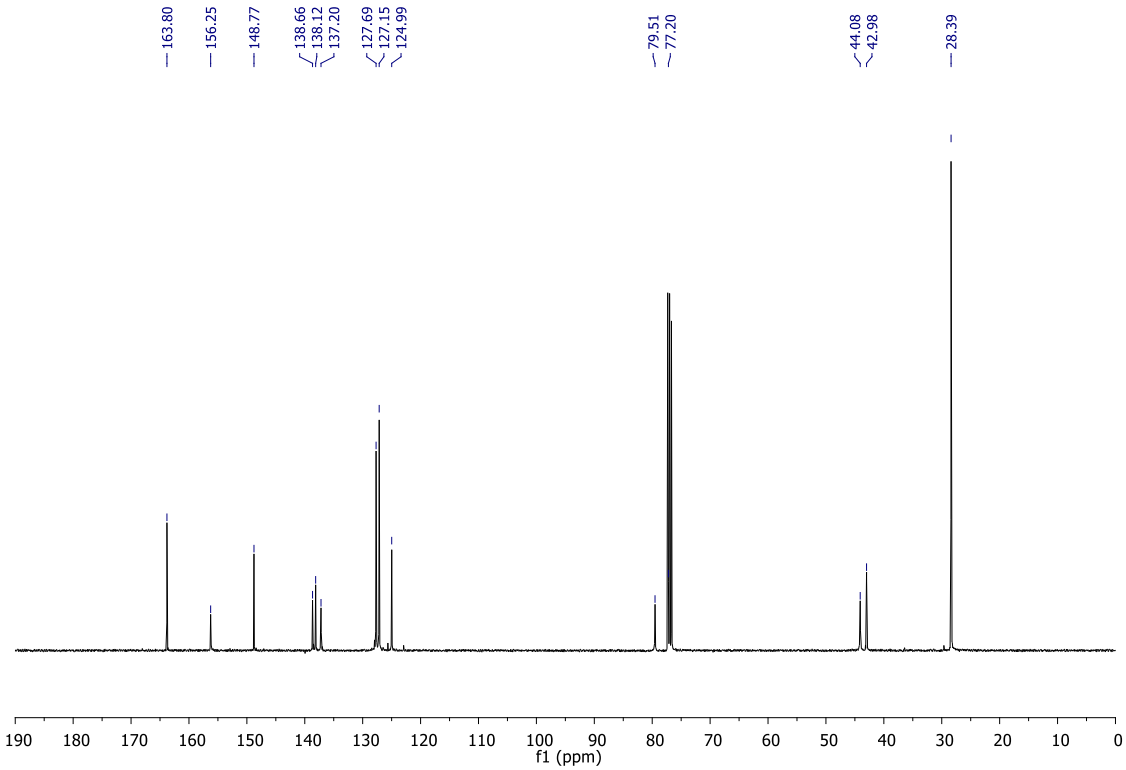
163.80
156.25
148.77
138.66
138.12
137.20
127.69
127.15
124.99
79.51
77.20
44.08
42.98
28.39
f1 (ppm)

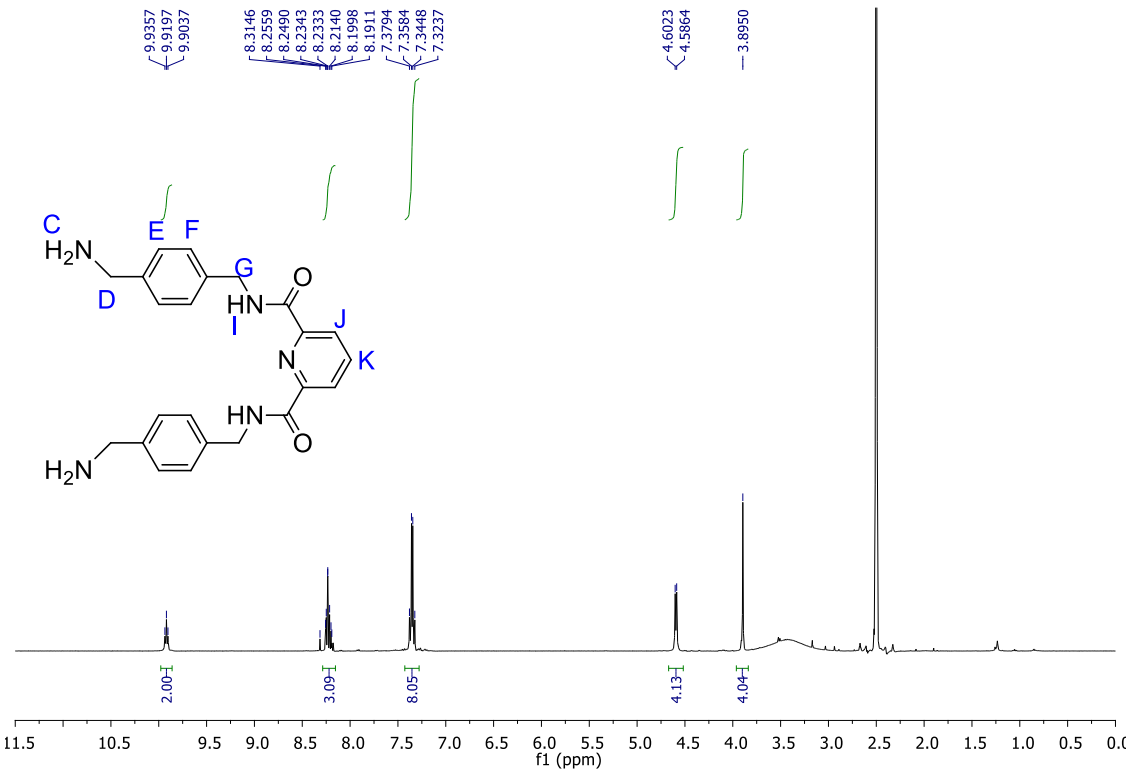
9.9357
9.9197
9.9037
8.3146
8.2559
8.2490
8.2343
8.2333
8.2140
8.1998
8.1911
7.3794
7.3584
7.3448
7.3237
4.6023
4.5864
3.8950
C
E
F
G
D
I
J
K
O
HN
N
H2N
2.00
3.09
8.05
4.13
4.04
f1 (ppm)

[2]Rotaxane

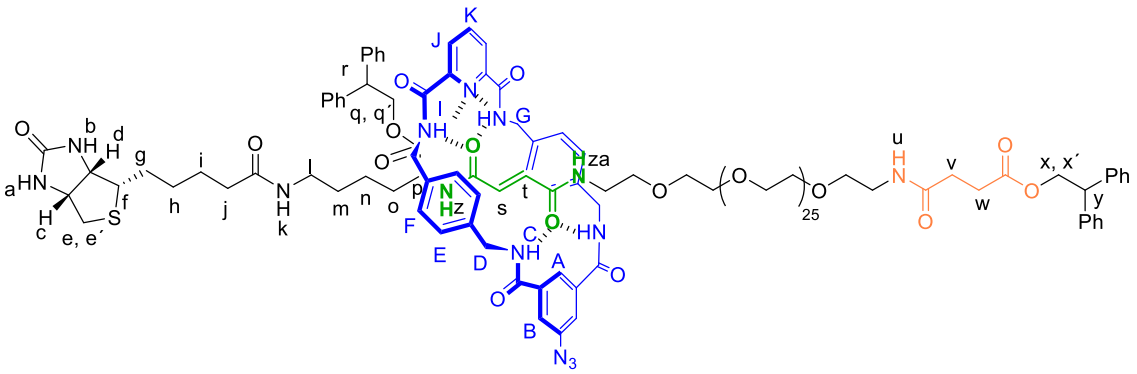

Compound 15

Thread **12** (16 mg, 7.3 x 10^{-3} mmol), was dissolved in 1.5 mL $CHCl_3$ (stabilized with amylenes), Et_3N (30 μL, 0.22 mmol) was added and the reaction mixture were stirred vigorously while solutions of the diamine, compound **14**, (36 mg, 0.09 mmol) in $CHCl_3$ (0.7 mL) and the acid chloride, compound **13** (21 mg, 0.09 mmol) in $CHCl_3$ (0.7 mL) were simultaneously added over a period of 3h using motor-driven syringe pumps. After 24h the resulting suspension was filtered and the solvent removed under reduced pressure. The crude material was purified by column chromatography (gradient elution: DCM/ MeOH 25:1 to 18:1) to furnish rotaxane **15** as a colorless oil (7 mg, 35%); ^{1}H NMR ([D6]dimethyl sulfoxide): δ = 9.83 (m, 1H, NH), 9.56 (m, 2H, NH), 9.18 M (m, 1H, NH), 8.72 (d, *J* = 7.1 Hz, 1H, NH_t or NH_z), 8.52 (t, *J* = 5.7 Hz, 1H, NH_z or NH_{za}), 8.31 (m, 1H, Ar-H), 8.22 (m, 2H, Ar-H), 8.11 (m, 1H, NH), 7.82 (m, 1H, NH), 7.70 (m, 1H, NH), 7.63 (m, 2H, Ar-H), 7.28 (m, 16 H, Ar-H), 7.21 (m, 8H, Ar-H), 7.13 (m, 4 H, Ar-H), 6.51 (m, 2H, H_s, H_t), 6.41 (br s, 1 H, H_a), 6.35 (br s, 1 H, H_b), 4.72 (dd, *J* = 8.1, 10.9 Hz, 1 H, H_q or $H_{q'}$), 4.56 (m, 7H, $H_{q'}$ or H_q, H_x, $H_{x'}$ and H_D or H_G), 4.37 (m, 7H, H_c, H_y, H_r and H_D or H_G), 4.11 (m, 2H, H_d, H_p), 3.50 (m, 14H, EG26-H), 3.40 (m, 90H, EG26-H), 3.17 (m, 2H, EG26-H), 3.08 (m, 1H, H_f), 2.91 (m, 2 H, H_l), 2.81 (m, 1 H, H_e or $H_{e'}$), 2.54 (d, *J* = 12.8 Hz, 1 H, $H_{e'}$ or H_e), 2.32 (m, 2 H, H_w), 2.21 (t, *J* = 6.6 Hz, 2 H, H_v), 2.03 (t, *J* = 6.8 Hz, 2 H, H_j), 1.44 (m, 12 H, H_g, H_i, H_h, H_n, H_m, H_o) MS m/z: calculated for $C_{108}H_{172}N_6O_{36}S$ $[M+Na]^+$ 2759.4 found MALDI-TOF 2763.3.

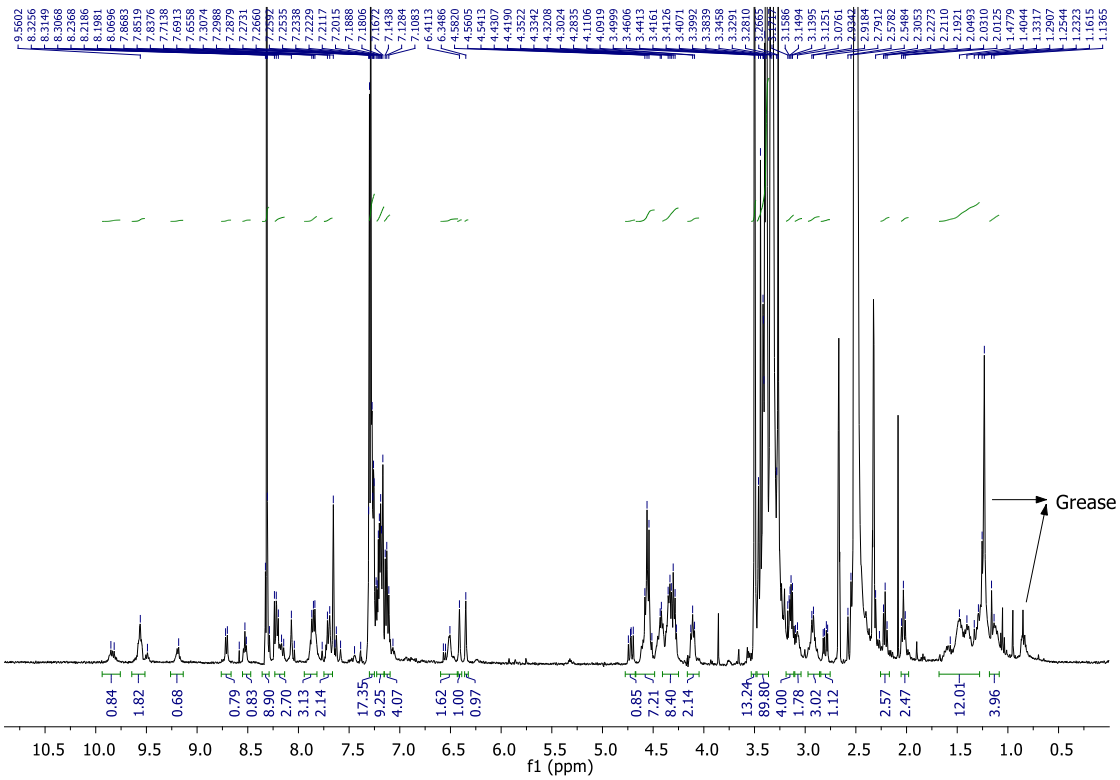
Grease
f1 (ppm)

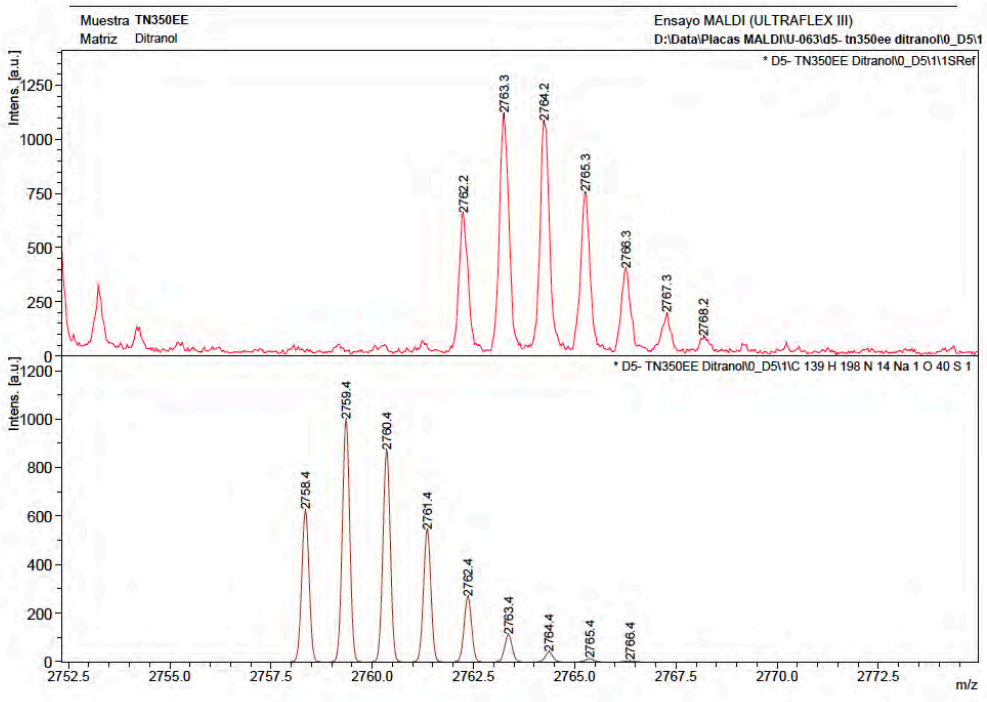
Muestra TN350EE
Matriz Ditranol
Ensayo MALDI (ULTRAFLEX III)
D:\Data\Placas MALDI\U-063\d5- tn350ee ditranol\0_D5\1
* D5- TN350EE Ditranol\0_D5\1\1SRef
* D5- TN350EE Ditranol\0_D5\1\C 139 H 198 N 14 Na 1 O 40 S 1
Intens. [a.u.]
m/z

Position of the macrocycle in solution

Comparison of the ^{1}H NMR spectra of thread, compound **12**, and [2]rotaxane compound **15** (depicted in the next two figures) in [D6]dimethyl sulfoxide (400 MHz, 298K) indicates that the macrocycle predominantly resides over the fumaramide station. The H_s and H_t protons of the fumaramide group are strongly shielded in the rotaxane compared to the thread evidenced by a shift in their peak positions by 0.34 ppm, whereas the chemical shifts of the H_v and H_w protons of the succinic amide-ester group are only slightly shifted by 0.05 ppm.

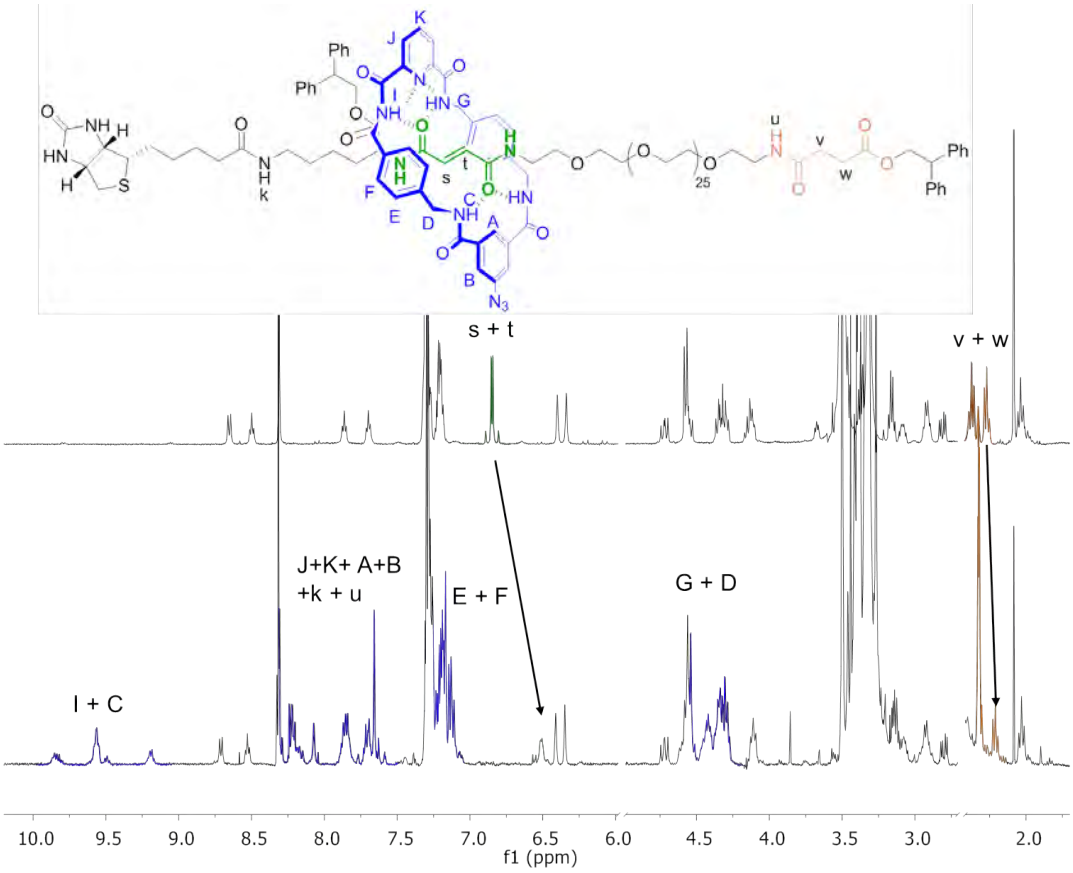

The figure above compares compound **12**, (*E*)-thread, (top spectrum) and compound **15**, rotaxane molecule, (bottom spectrum) Showing in green the protons corresponding to the fumaramide double bond, which are shifted in 0.34 ppm in the rotaxane molecule; in orange we can find the protons of the succinic-amide ester group, which are shifted only by 0.05 ppm in the rotaxane molecule. Finally we can find the protons corresponding to the macrocycle highlighted in blue.

S1.2 Oligonucleotide synthesis

The syntheses of oligonucleotides were performed on a MerMade 4 synthesizer (BioAutomation Corporation). For each oligonucleotide synthesis, columns were filled with the corresponding Controlled Pore Glass (CPG) solid support. Anhydrous MeCN was used as solvent. For the cleavage of DMTr protecting groups, the resin was purged with 3 % trichloroacetic acid in anhydrous DCM. The removal of the acid was carried out by purging with anhydrous MeCN. The activation of the phosphoramidite functionality was effected by a 0.25 M benzylthiotetrazole solution in anhydrous MeCN. The coupling time for standard phosphoramidites was 2 min and for cyclooctine derivative 5 min. Oxidation of P(III)-species was attained by alkaline iodine solution (20 mM I_2 in THF/Py/water 7/2/1). For the capping of residual 5'-OH-groups, a mixture of solution A (10% Ac_2O, 10% pyridine, 80% THF) and solution B (10% 1-methylimidazole in THF) was used. After completion of the synthesis, the oligonucleotides were cleaved from the solid support with concomitant removal of the Fmoc and β-cyanoethyl protecting groups by reacting the oligonucleotide-charged solid support with 28 % aq. NH_3 at 55 °C for 20 h. The solution was filtered and the filtrate was concentrated in vacuo. The residue was dissolved in 750 µL water. For purification of this crude oligonucleotide solution, a volume containing ~40 nmol crude oligonucleotide was applied to gel electrophoresis (1 mm, 20% polyacrylamide). The oligonucleotide-containing segments of the gel were visualized by UV-light (260 nm) and separated from the rest of the gel. Oligonucleotides were extracted from the gel using an elutrap system (3 h, 200 V). The solutions were desalted using a NAP-10 column and concentrated in an evaporating centrifuge.

Oligonucleotide 1

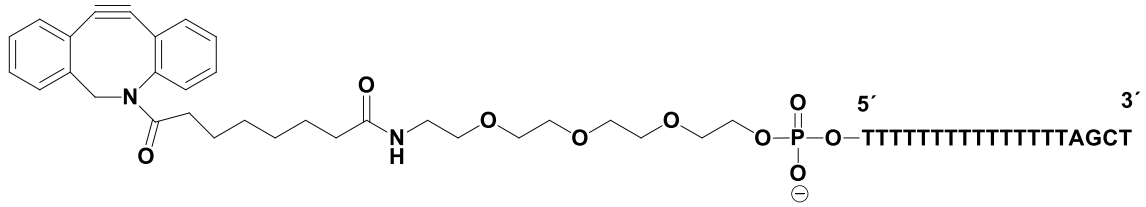

Oligonucleotide 2

3´ 5´
AAA AAA AAA AAA AAA

S1.3 Copper-free "click" reaction for coupling the macrocycle with a ssDNA oligonucleotide.

To a stirred solution of oligonucleotide 1 (50 μM) in H_2O/DMF (0.3 mL, 4/1) was added rotaxane 15 (60 μM) in H_2O/DMF (0.3 mL, 4/1). The mixture was allowed to stir overnight at room temperature. Followed and purified by gel electrophoresis (0.2 mm, 20% polyacrylamide). The oligonucleotide-containing segments of the gel were visualized by UV-light (260 nm) and separated from the rest of the gel. Oligonucleotides were extracted from the gel using an elutrap system (3 h, 200 V). The solutions were desalted using a NAP-10 column and concentrated in an evaporating centrifuge, to give the oligonucleotide 3.

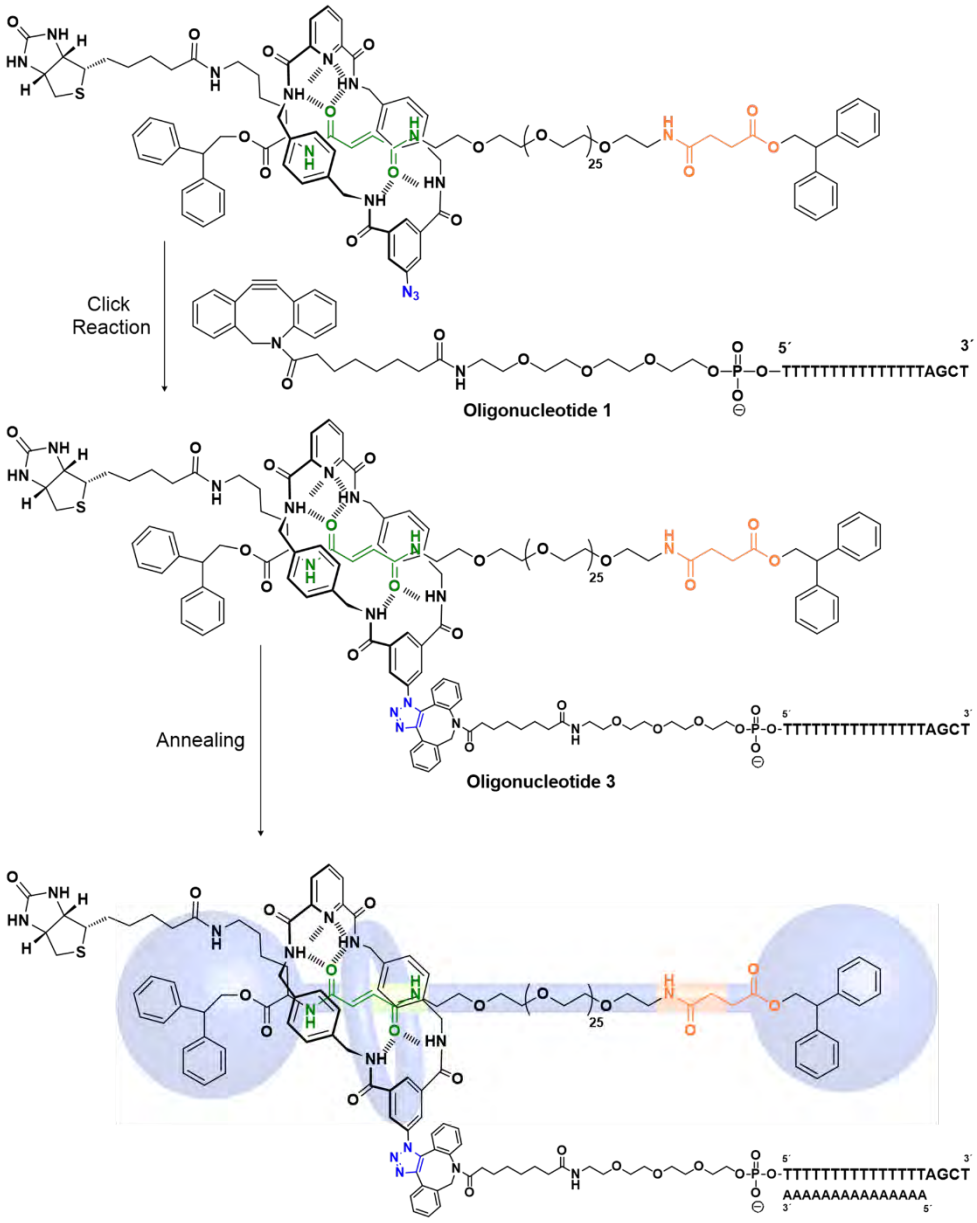

S1.4 Length of the oligoethyleneglycol thread

The theoretical length between the *fum* and *succ* stations of the relaxed thread in the gas phase was calculated as 11.2 nm by geometry optimization with the molecular mechanics (MMF94s, Figure S1) by using Avogadro (Avogadro: an open-source molecular builder and visualization tool. Version 1.2.0 http://avogadro.cc/).(*1*)

S1.5 Coupling of the shuttle with DNA handles for manipulation in the optical tweezers

For the optical tweezers experiments a single shuttle was connected between two functionalized beads using two double-stranded DNA (dsDNA) spacers, Fig. 1B. The first dsDNA spacer (or dsDNA handle) connects the macrocycle with the bead in the optical trap. This dsDNA handle was attached to the macrocycle as follows: Briefly, we first obtained a rotaxane modified with a ssDNA oligonucleotide through a 1,2,3-triazole group in the macrocycle (see above). Then the oligonucleotide on the rotaxane was annealed with a complementary polydA oligonucleotide (oligo 2). Finally, a 2686 bp long dsDNA molecule containing a protruding TCGA 5'-end was ligated to the protruding AGCT 3'-end of the oligo-rotaxane construct. This dsDNA molecule was labelled with multiple digoxigenins (Dig) at the other end following standardized procedures (25). A shorter dsDNA molecule (830 bp), labelled with streptavidin in one end and Dig in the other, connects the biotin labelled stopper to an anti-Dig covered bead held by suction on a micropipette.

S1.6 Synthesis of DNA spacers

The 2686 dsDNA handle was derived from the puc19 vector (Novagen). The plasmid was cut with *BamHI* and *SacI* restriction endonucleases (NEB). The *BamHI* was labelled with multiple Dig (*2*). The 830 bp dsDNA spacer connecting the biotin labelled stopper to the bead on the micropipette was synthetized by PCR amplification of the poly-linker section of the puc19 vector with two DNA oligonucleotides: one labelled with biotin and the other with digoxigenin at the 5'-end. The spacer was then incubated with saturated amounts of streptavidin and attached to anti-digoxigenin covered polystyrene micron-beads (Spherotech, Co).

S1.7 Optical tweezers experiments

Optical tweezers experiments were performed with a highly stable miniaturized dual-beam optical tweezers (*3*), with a limiting spatial resolution of ≤1 nm. In the optical tweezers the molecular shuttle is attached between two beads thought two dsDNA molecules as described above and in the main text (Fig. 1). All force extension curves were obtained at a pulling rate of 200 nm s^{-1}. The number of cycles obtained per molecule range between 20 and 120. Constant force measurements were performed with a feed-back stabilized protocol capable of maintaining a preset force within ~0.05 pN by moving the beads closer or further apart. All experiments were performed under near-physiological conditions (20 mM Tris-HCl pH 7.5, 150 mM NaCl) at 22±1 ^{o}C and data was taken at 1 kHz.

S1.8 Data analysis

Residence time calculations: In the hopping experiments the residence times at each station were calculated by partitioning each trace into two states using a threshold set at the midpoint between the histogram peaks.

Fit to Bell-Evans theory: The shuttling rates from *fum* to *succ* station, k_{fum}, and its reverse k_{succ}, were found to depend exponentially on force (Fig 4). The Bell-Evans theory has been applied previously to determine the main parameters that characterize the force-dependent kinetic rates of the folding/unfolding transitions of other two-state molecules (*20-22*). According to the Bell-Evans model k_{fum}, and k_{succ} depend on force following:

$$k_{fum}(f) = k(0)\ \exp\left(\frac{f\ x_{fum}}{k_B T}\right)$$

$$k_{succ}(f) = k(0)\exp\left(\frac{\Delta G \quad - f\ x_{succ}}{k_B T}\right)$$

where f corresponds to the external force, $k(0)$ is the shuttling rate at zero force; x_{fum} and x_{succ} are the relative distances between the *fum* and *succ* stations to the transition state at $f_{1/2}$, respectively, and ΔG is the shuttling free-energy of the molecular switch at zero force, defined as as $\Delta G_w = f_{1/2} \cdot \Delta x$ (where Δx is the distance between the *fum* and *succ* stations).

Calculation of energy profiles: The shuttling potential energy profile at a given force can be computed according to Boltzmann distribution as follows: $E(x) = -k_B \mathrm{T} \cdot \ln\rho(x)$. The term

$\rho(x)$ corresponds to the probability distribution of an extension x, and was obtained from the extension distributions shown in Fig. 3C.

S2 Supplementary figures

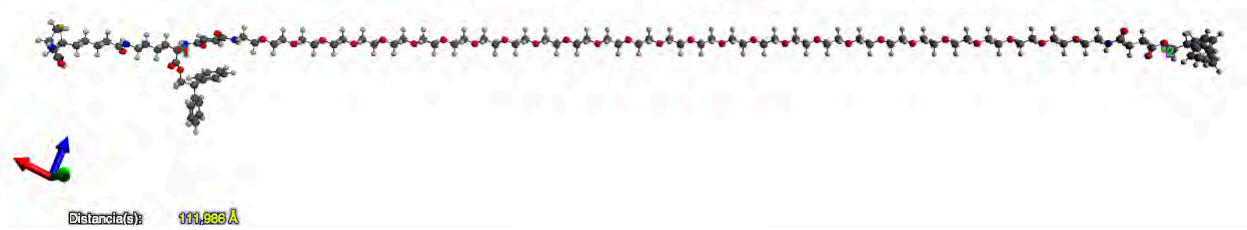

Fig. S1. Distance between stations in the gas phase. Energy-minimized (MMF94s structure of the thread, marking the distance between the N atom of the fum station (1) and the O atom of the succ station (2).

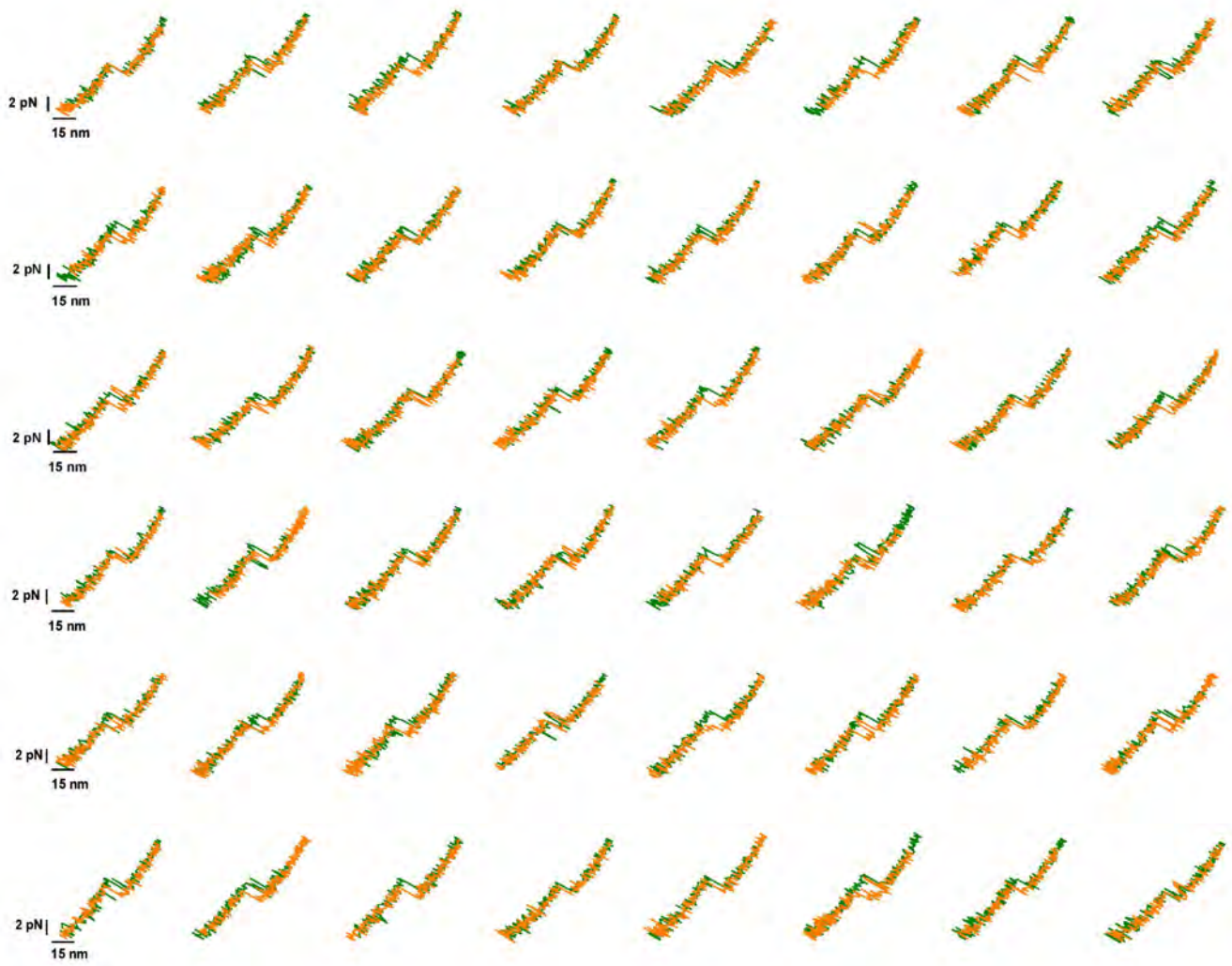

Fig. S2. Consecutive force-extension curves of a single rotaxane

The figure shows 48 consecutive pull (green)-relax (orange) cycles of a representative rotaxane-DNA construct (pulling rate 200 nm s^{-1}). Each pull-relax cycle is shown in an independent plot for clarity of display. The robustness of our method allowed us to obtain up to 120 pull-relax curves from a single molecule. The bi-stability of the molecule can be seen clearly in several curves as rapid oscillations of distance at forces close to $f_{1/2}$.

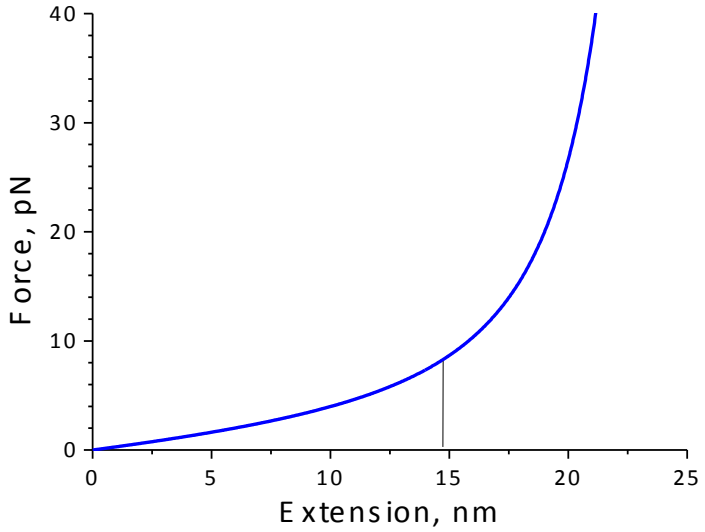

Fig. S3. Determination of the free energy of stretching of the rotaxane-DNA hybrid.

The force-extension curve of the rotaxane-DNA hybrid after shuttling, when the macrocycle is at the *succ* station, results from the elastic properties of the dsDNA (spacer and handle, 3615 bp) and those of the rotaxane. The Worm-Like-Chain model (WLC) of polymer elasticity is known to predict well both, the extension of dsDNA (*16*) and the extension of a linear polymer, like PEG (*4*), as a function of the applied force. In fact, the force-extension curve of the rotaxane-DNA hybrid after shuttling is well fit by an expression including the sum of two WLC models; one for the dsDNA, with persistence and contour lengths of L_p = 50 nm and L_c = 0.34 nm (16), respectively, and another for the rotaxane, with L_p = 0.9 ± 0.2 nm and L_c = 21.6 ± 1 nm, under our experimental conditions. The figure shows the force-extension curve of the rotaxane according to a WLC model including the L_p and L_c values determined from the fits. As expected, a length of 14.96 nm (indicated by a line) for the fully extended rotaxane at the coexistence force (8.61 pN) is predicted, which is fully compatible with the shuttling distance measured experimentally, ~15 nm. The free energy of stretching of the rotaxane ($\Delta G_{stretch}$) was calculated by integrating the area under the curve from 0 pN to the coexistence force, $\Delta G_{stretch}$= 11.8 k_BT.

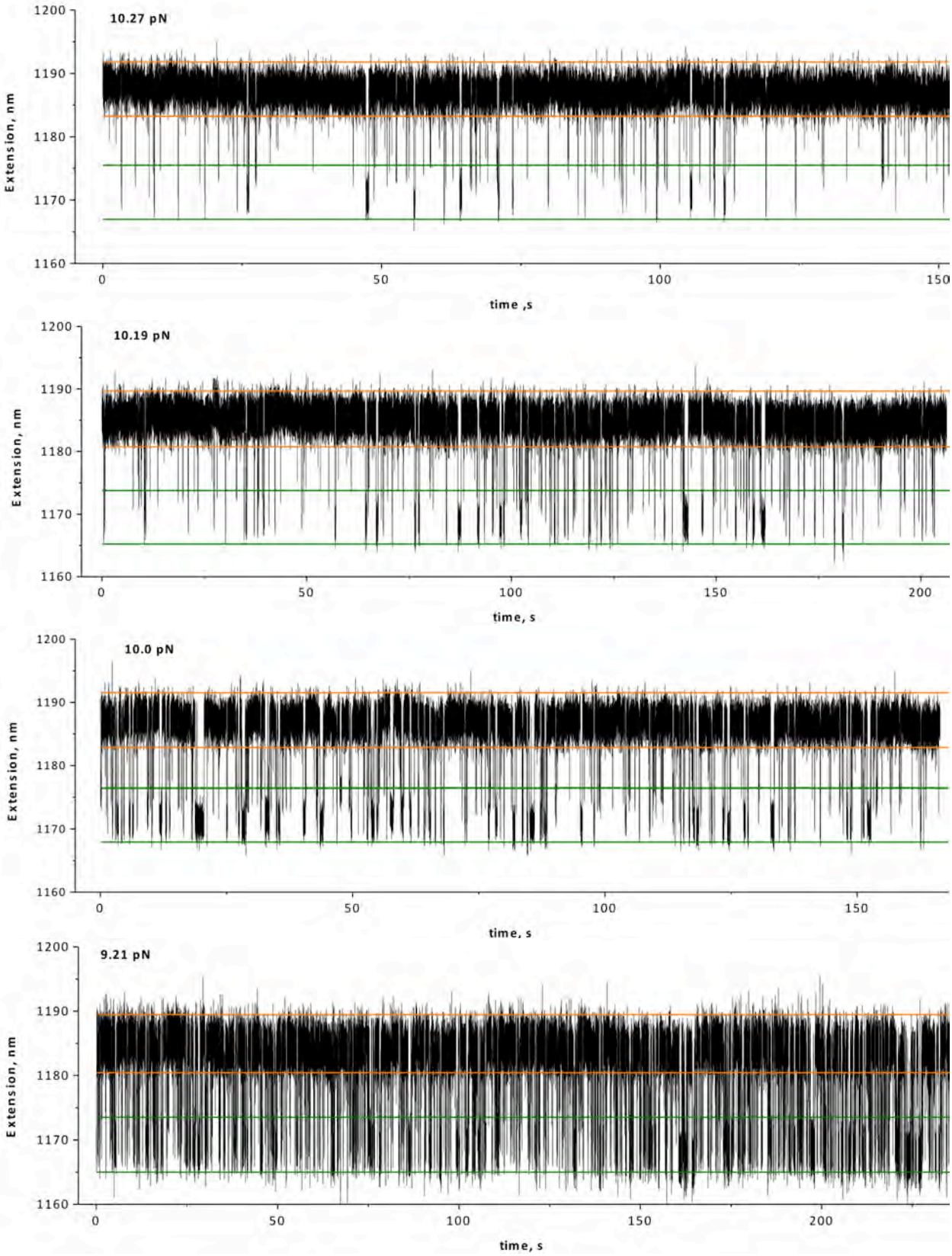
10.27 pN
Extension, nm
time ,s
10.19 pN
Extension, nm
time, s
10.0 pN
Extension, nm
time, s
9.21 pN
Extension, nm
time, s

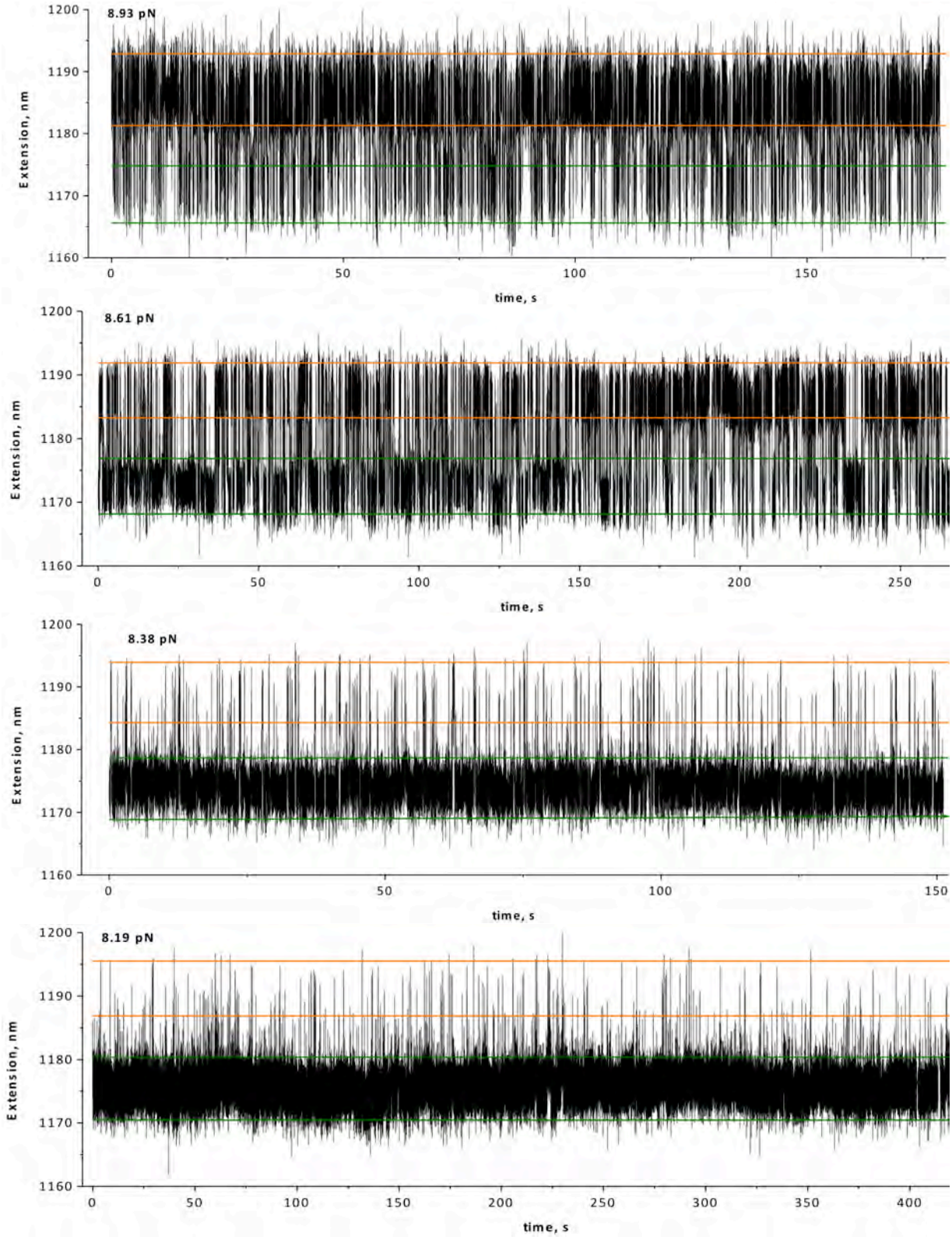

FigS4. Examples of the shuttling dynamics for independent rotaxane-DNA constructs at different constant forces. Green and orange lines represent the position of the *fum* and *succ* stations respectively. The extension axis shows the actual length of the rotaxane-DNA complex.

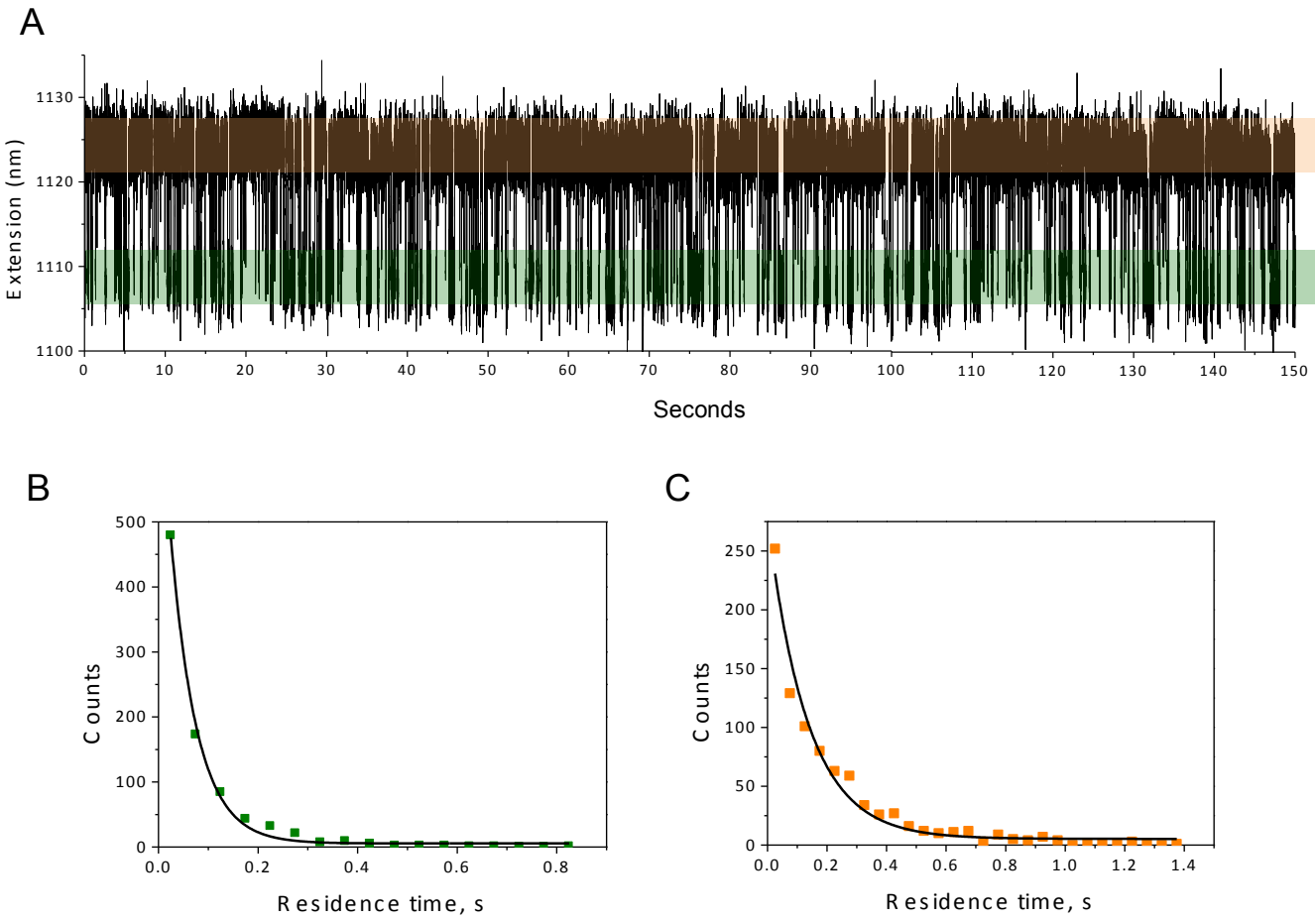

Fig S5. Distributions of residence times. (A) Real-time extension changes vs. time of a molecular shuttle hold at a constant force of 9.2 pN. For clarity of display only the first 150 seconds are shown (total recording time for this molecular shuttle was 240 s). Positions of the *fum* and *succ* stations are indicated in green and orange, respectively. (B) The residence time distribution at the *fum* station for molecule shown in (A) fits well to a single exponential (black line). (C) Residence time distribution at the *succ* station for molecule shown in (A) fitted to a single exponential (black line). As expected at force higher that $f_{1/2}$ the macrocycle spends longer times at the *succ* station.

References:

1. M. D. Hanwell et al., Avogadro: an advanced semantic chemical editor, visualization, and analysis platform. *J. Cheminform.* **4**, 17 (2012).

2. J.A. Morin, F.J. Cao, J.M. Lázaro, J.R. Arias-Gonzalez, J.M. Valpuesta, J.L. Carrascosa, M. Salas, B. Ibarra, Active DNA unwinding dynamics during processive DNA replication. *Proc. Natl. Acad. Sci. USA* **109**, 8115-8120 (2012).

3. J.M. Huguet, C.V. Bizarro, N. Forns, S.B. Smith, C. Bustamante, F. Ritort, Single-molecule derivation of salt dependent base-pair free energies in DNA. *Proc. Natl. Acad. Sci. USA* **107**, 15431-15436 (2010)

4. J.E. Mark, P.J. Flory, The configuration of the polyoxyethylene chain. *J .Am. Chem. Soc.* **87**, 1415-1423 (1965).